Induction of *p*-wave and *d*-wave order parameters in *s*-wave superconductors with light pulses

Hennadii Yerzhakov [1,*] and Alexander Balatsky [1,2,†]

[1]*Nordita, Stockholm University, and KTH Royal Institute of Technology, Hannes Alfvéns väg 12, SE-106 91 Stockholm, Sweden*

[2]*Department of Physics, University of Connecticut, Storrs, Connecticut 06269, USA*

(Received 7 April 2026; revised 10 August 2026; accepted 7 October 2026; published 9 November 2026)

We construct a generalized time-dependent Ginzburg-Landau model to demonstrate the possibility of inducing *p*- and *d*-wave components in an originally pure *s*-wave centrosymmetric superconductor via microwave radiation. In this framework, specializing to O_h point-group symmetry, we introduce gradient terms that couple the *s*-wave superconducting order parameter with other symmetry-allowed components. The singlet-to-singlet gradient terms are quadratic in spatial derivatives, while, in the presence of spin-orbit coupling, linear-in-derivatives terms coupling singlet and triplet order parameters are also permitted. Through the minimal substitution procedure, these terms enable coupling between different superconducting order parameters via the vector potential, thereby leading to the generation of *p*-wave, *d*-wave, and other symmetry-allowed components. Such a manipulation of the superconducting state locally via a microwave beam could be considered as one more facet of the concept of quantum printing.

DOI: 10.1103/gmxq-m8b4

I. INTRODUCTION

The interaction between superconducting (SC) condensates and electromagnetic (EM) radiation has been studied for several decades. One of the earliest indications that microwave radiation can enhance superconductivity came from experiments by Wyatt *et al.* [1] and Dayem and Wiegand [2], who observed microwave-enhanced critical currents in superconducting constrictions and thin-film bridges, respectively. Soon after, Eliashberg [3,4] developed a microscopic theory explaining the effect based on nonequilibrium redistribution of quasiparticles leading to an enhancement of the SC gap and allowing superconductivity to persist slightly above the equilibrium critical temperature T_c. Subsequent experiments on SC films measured an increase of T_c and the microwave-enhanced energy gap directly by tunneling further confirming Eliashberg's mechanism [5,6]. More recently, experiments employing intense THz pulses reported transient superconductinglike signatures at temperatures much higher than T_c [7–11]. Several theoretical mechanisms for the enhancement of SC have been proposed, including phonon-mediated enhancement of SC through the coherent excitation of lattice vibrations [12–15], while other studies have emphasized that accompanying heating effects may instead suppress superconductivity [16]. Alongside these efforts, increasing attention has been devoted to using electromagnetic radiation to coherently excite and control collective excitations of the superconducting condensate, including Higgs and Bardasis-Schrieffer modes [17–21], and to generate and control topological defects in the superconducting condensate [22–26]. Recent theoretical efforts have also been devoted to investigating the driving of the parent state into topologically nontrivial superconducting states [27,28], enhancement of preexisting unconventional correlations [29], and generation of unconventional superconducting correlations in initially conventional *s*-wave superconductors [21,30,31]. Induction of (even-frequency) triplet pairing is of particular interest, as it might provide new routes to topological superconductivity and control of spin-polarized SC currents. Our work belongs to this latter direction and develops a general symmetry-based framework for describing such light-induced order-parameter engineering in centrosymmetric *s*-wave superconductors.

In Ref. [21], based on a mix of microscopic and Ginzburg-Landau (GL) approaches, a theoretical proposal of switching the singlet *s*-wave superconducting state to a metastable triplet state in a superconductor on a honeycomb lattice with Kane-Mele spin-orbit coupling (SOC) [32] via tailored pulses of EM radiation is presented. The key ingredients in that paper are SOC and irradiation by an EM wave that breaks the inversion symmetry dynamically, i.e., there is no symmetry operation which is a combination of spatial inversion and time-shift operations. Importantly, the symmetry analysis of the model relied on the fact that Kane-Mele SOC reduces spin SU(2) symmetry to U(1), which leaves s_z, the z component of the spin, a good quantum number. However, for a generic centrosymmetric spin-orbit coupling in both two and three dimensions, none of the spin components is conserved. In this work, we generalize the symmetry-based time-dependent Ginzburg-Landau (TDGL) theory formulation to any centrosymmetric point group of the lattice in two- and three-dimensional (2D and 3D) cases. Additionally, we

*Contact author: yerzhako@ualberta.ca

†Contact author: alexander.balatsky@uconn.edu

Published by the American Physical Society under the terms of the Creative Commons Attribution 4.0 International license. Further distribution of this work must maintain attribution to the author(s) and the published article's title, journal citation, and DOI. Funded by Bibsam.

do not require dynamical inversion symmetry breaking as a necessary mechanism for inducing triplet correlations via EM radiation: The EM vector potential breaks inversion symmetry instantaneously, which in combination with SOC allows mixing of singlet and triplet components. In Ref. [30], the induction of triplet correlations by EM waves in an s-wave SC with SOC is studied within the Floquet-Magnus expansion. However, the models used in that work are for a noncentrosymmetric SC with Rashba-type spin-orbit coupling, which generically allows singlet-triplet admixture even in the absence of the external drive.

In this work, we construct a time-dependent GL theory concentrating on systems with O_h point-group symmetry, in which the s-wave order parameter (OP) is coupled to other symmetry-allowed singlet and triplet OPs via gradient terms. The key point of this work is the formulation of the Lifshitz-type invariant [33] (first order in spatial derivatives), which is allowed in the presence of SOC, coupling s- and p-wave SC OPs. Under EM irradiation, this coupling induces a dynamical p-wave component, whereas other gradient couplings generate additional singlet components.

Such dynamically induced singlet-triplet states might potentially provide a platform for Floquet-engineered topological superconductivity, induction of a transient topological superconducting state, and ultimately can lead to an alternative route to topological SC using light and microwave pulses to produce a p-wave SC. We can see that this route can have advantages as it does not require heterostructures with attendant disorder and imperfection effects. The proposed manipulation of the superconducting state with light represents another facet of quantum printing [24,25,34], in which the spatiotemporal structure of the light gauge potential modifies the superconducting state.

Although this work focuses on the Lifshitz-type invariant in the presence of a time-dependent vector potential, a possible implication in the static vector potential case is the emergence of triplet correlations in the vortex state of an originally s-wave superconductor at zero applied magnetic field [35]. This coupling may also be relevant for the explanation of the magnetic memory effect in 4Hb-TaS_2 [36,37].

The paper is structured as follows: In Sec. II, we recapitulate how the superconducting gap transforms under symmetry operations. In Sec. III, we construct a generalized time-dependent Ginzburg-Landau model for the O_h-symmetric crystal introducing gradient terms that couple the s-wave OP with the triplet p-wave and other singlet OPs. In Sec. IV, we derive equations of motion for the formulated model. In Sec. V, we present some analytical and numerical results on the induced superconducting components. Finally, we conclude in Sec. VI.

II. TRANSFORMATION PROPERTIES OF THE SUPERCONDUCTING GAP

The SC gap function for a single-band SC can generically be written as [38]

$$\hat{\Delta}(\boldsymbol{k}) = i[\sigma_0\psi(\boldsymbol{k}) + \boldsymbol{d}(\boldsymbol{k})\cdot\boldsymbol{\sigma}]\sigma_y, \tag{1}$$

where σ_0 is the 2×2 identity matrix and $\boldsymbol{\sigma} = (\sigma_x, \sigma_y, \sigma_z)$ is the vector of Pauli matrices. The terms with $\psi(\boldsymbol{k})$ and $\boldsymbol{d}(\boldsymbol{k})$ correspond to the singlet and triplet pairings, respectively. The group of symmetries is $\mathcal{G} = G\times \mathrm{SU}(2)\times\mathcal{T}\times \mathrm{U}(1)$ in the absence of SOC. This is reduced to $\mathcal{G} = G^D\times\mathcal{T}\times\mathrm{U}(1)$ in the presence of SOC. G is the space group of the lattice (we will concentrate on the corresponding point-group symmetry only), G^D is its double group, and $\mathcal{T}$ is the time-reversal symmetry. At the highest transition temperature in a centrosymmetric superconductor, either the singlet or the triplet component is nonzero. However, at lower temperatures, the ground state may exhibit singlet-triplet mixing [38–45].

In the absence of SOC, under the symmetry operations, the creation operators (in momentum space) transform as

$$\begin{aligned} g_O c^\dagger_{\boldsymbol{k},s} &= c_{D^-(g_O)\boldsymbol{k},s},\ g_S c^\dagger_{\boldsymbol{k}} = D_{1/2}(g_S)c_{\boldsymbol{k}},\\ \mathcal{T}c_{\boldsymbol{k}} &= -i\sigma_y c_{-\boldsymbol{k}},\ \Phi c_{\boldsymbol{k},s} = e^{i\phi}c_{\boldsymbol{k},s}, \end{aligned} \tag{2}$$

where g_O, g_S, and Φ are members of the symmetry groups G, SU(2), and U(1), respectively. $D^-(g)$ denote matrices in the three-dimensional odd representation of the group G. $D_{1/2}$ is the two-dimensional spin-$\frac{1}{2}$ representation of SU(2). Therefore, their actions on the gap function are

$$\begin{aligned} g_O\hat{\Delta}(\boldsymbol{k}) &= \hat{\Delta}(D^-(g_O)\boldsymbol{k}),\\ g_S\hat{\Delta}(\boldsymbol{k}) &= D_{1/2}(g_S)^T\hat{\Delta}(\boldsymbol{k})D_{1/2}(g_S),\\ \mathcal{T}\hat{\Delta}(\boldsymbol{k}) &= \sigma_y\hat{\Delta}(-\boldsymbol{k})^*\sigma_y,\ \Phi\hat{\Delta}(\boldsymbol{k}) = e^{2i\phi}\hat{\Delta}(\boldsymbol{k}). \end{aligned} \tag{3}$$

These operations can be rewritten for $\psi(\boldsymbol{k})$ and $\boldsymbol{d}(\boldsymbol{k})$ in Eq. (1):

$$\begin{aligned} g_O\psi(\boldsymbol{k}) &= \psi(D^-(g_O)\boldsymbol{k}),\ g_O\boldsymbol{d}(\boldsymbol{k}) = \boldsymbol{d}(D^-(g_O)\boldsymbol{k}),\\ g_S\psi(\boldsymbol{k}) &= \psi(\boldsymbol{k}),\ g_S\boldsymbol{d}(\boldsymbol{k}) = D^+(g_S)\boldsymbol{d}(\boldsymbol{k}),\\ \mathcal{T}\psi(\boldsymbol{k}) &= \psi(-\boldsymbol{k})^*,\ \mathcal{T}\boldsymbol{d}(\boldsymbol{k}) = -\boldsymbol{d}(-\boldsymbol{k})^*,\\ \Phi\psi(\boldsymbol{k}) &= e^{2i\phi}\psi(\boldsymbol{k}),\ \Phi\boldsymbol{d}(\boldsymbol{k}) = e^{2i\phi}\boldsymbol{d}(\boldsymbol{k}), \end{aligned} \tag{4}$$

where $D^+(g)$ are matrices in the even three-dimensional representation of G.

The presence of SOC "locks" rotations in spin and orbital spaces. Consequently, in this case

$$g_{OS}\hat{\Delta}(\boldsymbol{k}) = D^G_{1/2}(g_{OS})^T\hat{\Delta}(D^-(g_{OS})\boldsymbol{k})D^G_{1/2}(g_{OS}), \tag{5}$$

where $g_{OS}\in G^D$, $D^G_{1/2}$ is a 2×2 spinorial irrep of the double group G^D, and we instead have

$$\begin{aligned} g_{OS}\psi(\boldsymbol{k}) &= \psi(D^-(g_{OS})\boldsymbol{k}),\\ g_{OS}\boldsymbol{d}(\boldsymbol{k}) &= D^+(g_{OS})\boldsymbol{d}(D^-(g_{OS})\boldsymbol{k}). \end{aligned} \tag{6}$$

We want to investigate which couplings between OPs of different symmetries can be mediated by the electromagnetic vector potential, i.e., which gradient terms are allowed in the GL theory.

III. MODEL

A. SO(3) symmetry, no SOC

For continuous rotational symmetry, and even l, the gap function can be expanded in the basis functions of the $\mathcal{D}_l$

representation as

$$\hat{\Delta}(\boldsymbol{k}) = \sum_{m=-l}^{l} c_m Y_{lm}(\boldsymbol{k}) i\sigma_y = \sum_{m=-l}^{l} c_m \hat{\Delta}_m, \tag{7}$$

and for odd l

$$\hat{\Delta} = \sum_{m=-l}^{l} \sum_{\hat{n}=\hat{x},\hat{y},\hat{z}} c_{mn} Y_{lm}(\boldsymbol{k}) i(\boldsymbol{\sigma}\cdot\hat{n})\sigma_y. \tag{8}$$

Thus, the s wave is characterized by one coefficient $\hat{\Delta}_s(\boldsymbol{k}) = s\hat{\Delta}_s(\boldsymbol{k})$, and the p wave by nine coefficients

$$\hat{\Delta}_p = \sum_{i=1}^{3} \sum_{\alpha=\hat{x},\hat{y},\hat{z}} P_{i\alpha}\hat{\Delta}_{i\alpha}. \tag{9}$$

Transferring the transformation properties to the coefficients, we want to form an invariant that couples s and $P_{i\alpha}$ and contains derivatives that transform according to the $\mathcal{D}_1$ representation, i.e., their transformations are performed by applying regular SO(3) rotation matrices. We schematically (without specifying indices and numerical coefficients) write such a putative invariant and how it transforms as

$$I_\nabla = s\cdot\nabla^n P^m \underset{g_O,g_S}{\longrightarrow} s\cdot D^{-n}(g_O)\nabla^n D^{-m}(g_O)\cdot D^{+m}(g_S)P^m. \tag{10}$$

Since $D_\pm$ are simply rotation matrices for proper rotations, any polynomial constructed from them can be reduced to a constant by appropriately pairing indices and inserting Levi-Civita tensors ϵ_{ijk}, using $R^T R = \mathbb{1}$ and $\det R = 1$, where R is a rotation matrix. Thus, to form an invariant, we have to have an even number of $D^-(g_O)$ matrices to satisfy invariance under inversion and $m \geqslant 2$ to satisfy invariance under spin rotations. Within the TDGL model, such invariants provide terms of at least linear order in P to the TDGL equations, which will be zero as long as the p-wave components are zero. Therefore, such terms will be unable to induce the triplet component via microwave irradiation or via nonuniformity of the s-wave OP in the vortex state.

Note that couplings between singlet OPs of different symmetries, e.g., between s- and d-wave components, are allowed in second order in spatial derivatives and in first order in the OPs even without SOC.

B. SO(3) symmetry, SOC is present

The situation is different in the presence of SOC. After SOC is turned on, the full group SO(3) × SU(2) reduces to SU(2) (acting in combined spin and orbital space). Correspondingly, the irreducible representation, according to which the SC gap transformed in the case of no SOC, becomes a reducible representation of SU(2). Generically, under the SOC, the physical spin ceases to be a good quantum number for labeling energy-degenerate single-particle states, from which Cooper pairs are formed. Therefore, we switch to the appropriate pseudospin basis, in which the single-particle Hamiltonian is diagonalized. In this basis, the singlet and triplet components of the superconducting gap retain their symmetry-defined meaning under inversion, whereas in the physical spin basis the singlet and triplet components generally mix. The eigenbasis of the SC gap for even l now transforms according to

$$\mathcal{D}_l \otimes \mathcal{D}_0 = \mathcal{D}_l, \tag{11}$$

and for odd l as

$$\mathcal{D}_l \otimes \mathcal{D}_1 = \mathcal{D}_{l-1} \oplus \mathcal{D}_l \oplus \mathcal{D}_{l+1}. \tag{12}$$

Thus, for the p-wave component with $l = 1$, it is possible to form an invariant of the first order in both the spatial derivatives and the p-wave components $P_{i\alpha}$.

Specifically, such an invariant transforms under a g_{OS} operation as

$$\begin{aligned} I_\nabla &= a_{ij\alpha} s^* \partial_i P_{j\alpha} + \text{c.c.} \\ &\underset{g_{OS}}{\longrightarrow} a_{ij\alpha} s D^-_{ii'}(g_{OS})\partial_{i'} D^{-\ m}_{jj'}(g_{OS}) D^{+\ m}_{\alpha\alpha'}(g_{OS}) P_{j'\alpha'} + \text{c.c.}, \end{aligned} \tag{13}$$

where $a_{ij\alpha}$ are the coefficients to be determined. Since $D^- = D^+ i$, where $i = \pm 1$ depending on whether the operation is proper or improper rotation, and $\det D^+ = 1$ can be rewritten in the form

$$\epsilon_{ijk} D^+_{ii'} D^+_{jj'} D^+_{kk'} = \epsilon_{i'j'k'}, \tag{14}$$

where ϵ_{ijk} is the totally antisymmetric tensor, it is easy to see that $a_{ij\alpha} \sim \epsilon_{ij\alpha}$. Given that I_∇ is integrated over the volume in the Lagrangian, using integration by parts, it can be rewritten in an antisymmetric form

$$I_\nabla \sim \epsilon_{ij\alpha}[s^*\partial_i P_{j\alpha} - (\partial_i s^*)P_{j\alpha} + \text{c.c.}]. \tag{15}$$

An important feature of this Lifshitz-type term is that it introduces terms of zeroth order in $P_{i\alpha}$ to the equations of motion, which leads to the generation of the triplet component via application of periodic (electromagnetic wave) or static (constant magnetic field) vector potentials. The strength of coefficients $a_{ij\alpha}$ is expected to be proportional to the strength of the SOC in the first approximation. Linear in gradient terms of this type have been discussed in the context of noncentrosymmetric superconductors [46–50] and multiband superconductors [51–53]. For single-band centrosymmetric SCs, it was originally introduced in Ref. [46] within the GL framework, where the focus of the study was on helical SC states, and, to the best of our knowledge, was not discussed in the literature after that except in Ref. [35], where the generation of a triplet component in the vortex state of a d-wave SC was studied. In addition, while assumed, the importance of SOC was not discussed in Ref. [46]. It recently reappeared in Ref. [21], where it was microscopically derived for a specific model on a honeycomb lattice with Kane-Mele spin-orbit coupling [32].

C. O_h symmetry with SOC

We proceed by constructing a theory for the case of cubic symmetry with inversion center O_h and nonzero SOC. O_h has five even and five odd representations, with the corresponding basis functions given in Table I. The gap function in the Γ

TABLE I. Irreducible representations and their corresponding basis functions $\hat{\Delta}^i_\Gamma$ [38]. For even irreps, $\hat{\Delta}^i_\Gamma = i\sigma_y\psi_\Gamma(\boldsymbol{k})$, and for odd irreps $\hat{\Delta}^i_\Gamma = i[\boldsymbol{\sigma}\cdot\boldsymbol{d}^i_\Gamma(\boldsymbol{k})]\sigma_y$.

Irrep Γ	Basis functions	Irrep Γ	Basis vector functions
A_{1g}	$\psi_{A_{1g}}(k) = 1,\ k_x^2+k_y^2+k_z^2$	A_{1u}	$d_{A_{1u}}(k) = \hat{x}k_x + \hat{y}k_y + \hat{z}k_z$
A_{2g}	$\psi_{A_{2g}}(k) = (k_z^2-k_y^2)(k_y^2-k_x^2)(k_z^2-k_x^2)$	A_{2u}	$d_{A_{2u}}(k) = \hat{x}k_x(k_z^2-k_y^2) + \hat{y}k_y(k_x^2-k_z^2) + \hat{z}k_z(k_y^2-k_x^2)$
E_g	$[t]\psi^1_{E_g}(k) = 2k_z^2-k_x^2-k_y^2,\ \ \psi^2_{E_g}(k) = \sqrt{3}(k_x^2-k_y^2)$	E_u	$d^1_{E_u,}(k) = 2\hat{z}k_z - \hat{x}k_x - \hat{y}k_y,\ d^2_{E_u}(k) = \sqrt{3}(\hat{x}k_x - \hat{y}k_y)$
T_{1g}	$[t]\psi^1_{T_{1g}}(k) = k_yk_z(k_y^2-k_z^2),\ \psi^2_{T_{1g}}(k) = k_zk_x(k_z^2-k_x^2),\ \psi^3_{T_{1g}}(k) = k_xk_y(k_x^2-k_y^2)$	T_{1u}	$d^1_{T_{1u}}(k) = \hat{y}k_z - \hat{z}k_y,\ d^2_{T_{1u}}(k) = \hat{z}k_x - \hat{x}k_z,\ d^3_{T_{1u}}(k) = \hat{x}k_y - \hat{y}k_x$
T_{2g}	$[t]\psi^1_{T_{2g}}(k) = k_yk_z,\ \psi^2_{T_{2g}}(k) = k_zk_x,\ \psi^3_{T_{2g}}(k) = k_xk_y$	T_{2u}	$d^1_{T_{2u}}(k) = \hat{y}k_z + \hat{z}k_y,\ d^2_{T_{2u}}(k) = \hat{z}k_x + \hat{x}k_z,\ d^3_{T_{2u}}(k) = \hat{x}k_y + \hat{y}k_x$

representation can be written as

$$\hat{\Delta} = \sum_{i=1}^{d_\Gamma} \eta^i_\Gamma \hat{\Delta}^i_\Gamma, \tag{16}$$

where d_Γ is the dimension of the representation Γ.

1. A_{1g} to triplet

We start by forming invariants linear in gradient, singlet (*s*-wave) A_{1g} OP, and triplet OPs. Using the direct product table, Table IV [54,55] in Appendix A, we find that the only such coupling is between A_{1g} (*s*-wave) and T_{1u} (*p*-wave) irreps. Indeed, given that the components of $\boldsymbol{\nabla}$ transform according to T_{1u} irrep, for the invariant term of the structure $(\eta_{A_{1g}})^*(\boldsymbol{\nabla}\eta_{\Gamma_u})$ to exist, there should be a trivial irrep in the decomposition of $A_{1g}\otimes T_{1u}\otimes\Gamma_u$. Using a theorem that a direct product of

TABLE II. Lifshitz-type invariants coupling *s*-wave OP with symmetry-allowed triplet OPs in different centrosymmetric crystallographic point groups.

Group	Lifshitz-type invariants
C_i	$\eta^*_{A_g}\partial_x\eta_{A_u} - (\partial_x\eta^*_{A_g})\eta_{A_u}$+ c.c. $\eta^*_{A_g}\partial_y\eta_{A_u} - (\partial_y\eta^*_{A_g})\eta_{A_u}$+ c.c. $\eta^*_{A_g}\partial_z\eta_{A_u} - (\partial_z\eta^*_{A_g})\eta_{A_u}$+ c.c.
C_{2h}	$\eta^*_{A_g}\partial_x\eta_{B_u} - (\partial_x\eta^*_{A_g})\eta_{B_u}$+ c.c. $\eta^*_{A_g}\partial_y\eta_{B_u} - (\partial_y\eta^*_{A_g})\eta_{B_u}$+ c.c. $\eta^*_{A_g}\partial_z\eta_{A_u} - (\partial_z\eta^*_{A_g})\eta_{A_u}$+ c.c.
D_{2h}	$\eta^*_{A_g}\partial_x\eta_{B_{3u}} - (\partial_x\eta^*_{A_g})\eta_{B_{3u}}$+ c.c. $\eta^*_{A_g}\partial_y\eta_{B_{2u}} - (\partial_y\eta^*_{A_g})\eta_{B_{2u}}$+ c.c. $\eta^*_{A_g}\partial_z\eta_{B_{1u}} - (\partial_z\eta^*_{A_g})\eta_{B_{1u}}$+ c.c.
C_{4h} S_6 (or C_{3i})	$\eta^*_{A_g}(\partial_x\eta^1_{E_u} + \partial_y\eta^2_{E_u}) - ((\partial_x\eta^*_{A_g})\eta^1_{E_u} + (\partial_y\eta^*_{A_g})\eta^2_{E_u})$+ c.c. $\eta^*_{A_g}(\partial_x\eta^2_{E_u} - \partial_y\eta^1_{E_u}) - ((\partial_x\eta^*_{A_g})\eta^2_{E_u} - (\partial_y\eta^*_{A_g})\eta^1_{E_u})$+ c.c. $\eta^*_{A_g}\partial_z\eta_{A_u} - (\partial_z\eta^*_{A_g})\eta_{A_u}$+ c.c.
D_{4h} D_{3d}	$\eta^*_{A_{1g}}(\partial_x\eta^1_{E_u} + \partial_y\eta^2_{E_u}) - ((\partial_x\eta^*_{A_{1g}})\eta^1_{E_u} + (\partial_y\eta^*_{A_{1g}})\eta^2_{E_u})$+ c.c. $\eta^*_{A_{1g}}\partial_z\eta_{A_{2u}} - (\partial_z\eta^*_{A_{1g}})\eta_{A_{2u}}$+ c.c.
C_{6h}	$\eta^*_{A_g}(\partial_x\eta^1_{E_{1u}} + \partial_y\eta^2_{E_{1u}}) - ((\partial_x\eta^*_{A_g})\eta^1_{E_{1u}} + (\partial_y\eta^*_{A_g})\eta^2_{E_{1u}})$+ c.c. $\eta^*_{A_g}(\partial_x\eta^2_{E_{1u}} - \partial_y\eta^1_{E_{1u}}) - ((\partial_x\eta^*_{A_g})\eta^2_{E_{1u}} - (\partial_y\eta^*_{A_g})\eta^1_{E_{1u}})$+ c.c. $\eta^*_{A_g}\partial_z\eta_{A_u} - (\partial_z\eta^*_{A_g})\eta_{A_u}$+ c.c.
D_{6h}	$\eta^*_{A_{1g}}(\partial_x\eta^1_{E_{1u}} + \partial_y\eta^2_{E_{1u}}) - ((\partial_x\eta^*_{A_{1g}})\eta^1_{E_{1u}} + (\partial_y\eta^*_{A_{1g}})\eta^2_{E_{1u}})$+ c.c. $\eta^*_{A_{1g}}\partial_z\eta_{A_{2u}} - (\partial_z\eta^*_{A_{1g}})\eta_{A_{2u}}$+ c.c.
T_h	$\eta^*_{A_g}(\partial_x\eta^1_{T_u} + \partial_y\eta^2_{T_u} + \partial_z\eta^3_{T_u}) - ((\partial_x\eta^*_{A_g})\eta^1_{T_u} + (\partial_y\eta^*_{A_g})\eta^2_{T_u} + (\partial_z\eta^*_{A_g})\eta^3_{T_u})$+ c.c.
O_h	$\eta^*_{A_{1g}}(\partial_x\eta^1_{T_{1u}} + \partial_y\eta^2_{T_{1u}} + \partial_z\eta^3_{T_{1u}}) - ((\partial_x\eta^*_{A_{1g}})\eta^1_{T_{1u}} + (\partial_y\eta^*_{A_{1g}})\eta^2_{T_{1u}} + (\partial_z\eta^*_{A_{1g}})\eta^3_{T_{1u}})$+ c.c.

two real irreps contains a trivial one if and only if those two irreps coincide [56], we see that such an invariant can be formed only if $\Gamma_u = T_{1u}$. For an O_h point group, it is given by Eq. (21). In Table II, we list Lifshitz-type invariants coupling s-wave OP with the symmetry-allowed triplet OPs for all crystallographic point groups.

2. A_{1g} to singlet

The couplings between s-wave and other singlet components need at least two gradients to form an invariant. Decomposing direct products (showing only the A_{1g} irrep and using ellipses for all other terms) $A_{1g} \otimes T_{1u} \otimes T_{1u} \otimes \Gamma_g$, using Table IV,

$$A_{1g} \otimes T_{1u} \otimes T_{1u} \otimes \begin{pmatrix} A_{1g} \\ A_{2g} \\ E_g \\ T_{1g} \\ T_{2g} \end{pmatrix} = \begin{pmatrix} A_{1g} + \cdots \\ \cdots \\ A_{1g} + \cdots \\ A_{1g} + \cdots \\ A_{1g} + \cdots \end{pmatrix}, \tag{17}$$

we find that couplings to all other singlets, except for A_{2g}, are possible. Again, because such terms are linear in η_{Γ_g}, such invariants will yield terms independent of η_{Γ_g} in the TDGL equations, and thus capable of inducing those components via application of periodic or static vector potentials. In the case of the latter one, in Ref. [57] it has been shown that subdominant d-wave OP might nucleate in the vicinity of the s-wave vortices and lead to type-1.5 superconductivity.

Together, the s-wave (A_{1g}) OP could be coupled via vector potential to the T_{1u} (p-wave), E_g ($d_{x^2-y^2}$ and d_{z^2}), T_{1g} (g-wave), and T_{2g} (d_{xy}, d_{xz}, and d_{yz}) OPs. We thus also investigate possible couplings between them. The schematic picture showing possible gradient couplings between different SC components in the constructed GL theory is illustrated in Fig. 1.

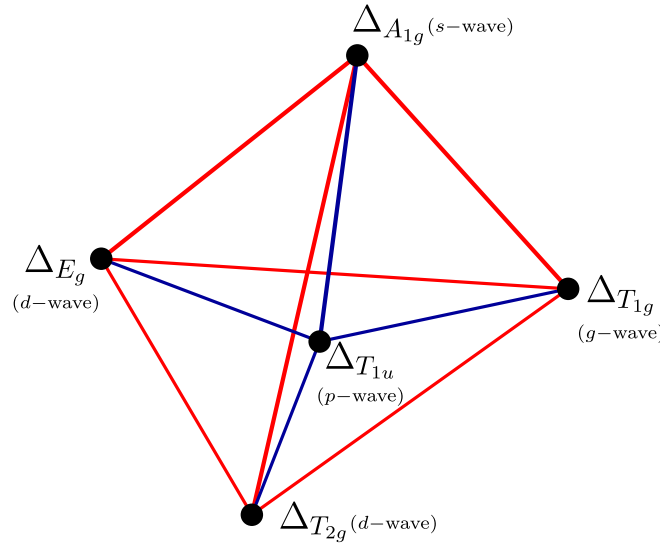


FIG. 1. Schematic diagram of gradient couplings between different SC OPs. Red and blue colors stand for the singlet-to-singlet and singlet-to-triplet couplings, respectively. Thicker lines correspond to couplings to the s-wave OP, which is the only nonzero OP in the absence of the vector potential.

D. Lagrangian

The full static Lagrangian density is thus

$$\mathcal{L}_{st} = \sum_{\Gamma\in\Gamma_r} \mathcal{L}_\Gamma + \sum_{\Gamma\in\Gamma_r}{}' \mathcal{L}_{A_{1g}\Gamma} + \mathcal{L}_{T_{1u}E_g} + \mathcal{L}_{T_{1u}T_{1g}}\mathcal{L}_{T_{1u}T_{2g}} + \mathcal{L}_{E_gT_{1g}} + \mathcal{L}_{E_gT_{2g}} + \mathcal{L}_{T_{1g}T_{2g}}, \tag{18}$$

where Γ_r is the set of T_{1u} and all even irreps of the group, excluding A_{2g}, and the prime in the superscript of the sum means excluding A_{1g} from the sum. $\mathcal{L}_\Gamma$'s are given by [38]

$$\mathcal{L}_{A_{1g}} = r_{A_{1g}} |\eta_{A_{1g}}|^2 + \sum_i a_{A_{1g}} |D_i \eta_{A_{1g}}|^2 + b_{A_{1g}} |\eta_{A_{1g}}|^4, \tag{19}$$

$$\begin{aligned}
\mathcal{L}_{T_{1u}} = {} & r_{T_{1u}} \sum_{i=1}^{3} |\eta^i_{T_{1u}}|^2 + a^1_{T_{1u}} \sum_{i=1}^{3} |D_i \eta^i_{T_{1u}}|^2 + a^2_{T_{1u}} \left(|D_x \eta^2_{T_{1u}}|^2 + |D_x \eta^3_{T_{1u}}|^2 + |D_y \eta^1_{T_{1u}}|^2 + |D_y \eta^3_{T_{1u}}|^2 + |D_z \eta^1_{T_{1u}}|^2 + |D_z \eta^2_{T_{1u}}|^2\right) \\
& + a^3_{T_{1u}} \left[(D_x \eta^1_{T_{1u}})^* (D_y \eta^2_{T_{1u}}) + (D_y \eta^2_{T_{1u}})^* (D_z \eta^3_{T_{1u}}) + (D_z \eta^3_{T_{1u}})^* (D_x \eta^1_{T_{1u}}) + \text{c.c.}\right] \\
& + a^4_{T_{1u}} \left[(D_x \eta^2_{T_{1u}})^* (D_y \eta^1_{T_{1u}}) + (D_y \eta^3_{T_{1u}})^* (D_z \eta^2_{T_{1u}}) + (D_z \eta^1_{T_{1u}})^* (D_x \eta^3_{T_{1u}}) + \text{c.c.}\right] \\
& + b^1_{T_{1u}} \left(\sum_{i=1}^{3} |\eta^i_{T_{1u}}|^2\right)^2 + b^2_{T_{1u}} \left|\sum_{i=1}^{3} (\eta^i_{T_{1u}})^2\right|^2 + b^3_{T_{1u}} \left(|\eta^1_{T_{1u}}|^2 |\eta^2_{T_{1u}}|^2 + |\eta^1_{T_{1u}}|^2 |\eta^3_{T_{1u}}|^2 + |\eta^2_{T_{1u}}|^2 |\eta^3_{T_{1u}}|^2\right), \\
\mathcal{L}_{E_g} = {} & r_{E_g} \sum_{i=1}^{2} |\eta^i_{E_g}|^2 + a^1_{E_g} \sum_{j=1}^{3} \sum_{i=1}^{2} |D_j \eta^i_{E_g}|^2 + b^1_{E_g} \left(\sum_{i=1}^{2} |\eta^i_{E_g}|^2\right)^2 + b^2_{E_g} \left(\eta^{1*}_{E_g} \eta^2_{E_g} - \eta^{2*}_{E_g} \eta^1_{E_g}\right)^2 \\
& + a^2_{E_g} \{2\left(|D_z \eta^2_{E_g}|^2 - |D_z \eta^1_{E_g}|^2\right) - \left(|D_x \eta^1_{E_g}|^2 - |D_x \eta^2_{E_g}|^2\right) - \left(|D_y \eta^1_{E_g}|^2 - |D_y \eta^2_{E_g}|^2\right) \\
& + \sqrt{3} \left((D_x \eta^1_{E_g})(D_x \eta^2_{E_g})^* - (D_y \eta^1_{E_g})(D_y \eta^2_{E_g})^* + \text{c.c.}\right)\}, \\
\mathcal{L}_{T_{1g}} = {} & \mathcal{L}_{T_{1u}}|_{T_{1u}\to T_{1g}}, \quad \mathcal{L}_{T_{2g}} = \mathcal{L}_{T_{1u}}|_{T_{1u}\to T_{2g}},
\end{aligned} \tag{20}$$

where $D_i = \partial_i - i2e/\hbar \cdot A_i$ is the covariant derivative, and e is the electron charge. Representing the terms that couple A_{1g} with other irreps as the sum of the gradient and uniform parts, $L_{A_{1g}\Gamma} = L_{A_{1g}\Gamma}{}^{\nabla} + L_{A_{1g}\Gamma}{}^{u}$, for the gradient parts, we obtain

$$\mathcal{L}^{\nabla}_{A_{1g},T_{1u}} = a_{A_{1g}T_{1u}} \sum_{i=1}^{3} \left\{ \eta^{*}_{A_{1g}} D_i \eta^{i}_{T_{1u}} - \left(D_i \eta_{A_{1g}}\right)^{*} \eta^{i}_{T_{1u}} + \text{c.c.} \right\}, \tag{21}$$

$$\begin{aligned}\mathcal{L}^{\nabla}_{A_{1g},E_g} = a_{A_{1g}E_g} \Big\{ & \tfrac{1}{2}\left(D_x \eta^{1}_{E_g}\right)^{*} D_x \eta_{A_{1g}} - \tfrac{1}{2}\left(D_x \eta^{2}_{E_g}\right)^{*} D_x \eta_{A_{1g}} - \tfrac{1}{2}\left(D_y \eta^{1}_{E_g}\right)^{*} D_y \eta_{A_{1g}} \\ & - \tfrac{1}{2}\left(D_y \eta^{2}_{E_g}\right)^{*} D_y \eta_{A_{1g}} + \left(D_z \eta^{2}_{E_g}\right)^{*} D_z \eta_{A_{1g}} + \text{c.c.} \Big\},\end{aligned} \tag{22}$$

$$\begin{aligned}\mathcal{L}^{\nabla}_{A_{1g},T_{1g}} = a_{A_{1g}T_{1g}} \Big\{ & - D_x \eta_{A_{1g}} \left(D_y \eta^{1}_{T_{1g}}\right)^{*} + D_y \eta_{A_{1g}} \left(D_x \eta^{1}_{T_{1g}}\right)^{*} - D_x \eta_{A_{1g}} \left(D_z \eta^{2}_{T_{1g}}\right)^{*} \\ & + D_z \eta_{A_{1g}} \left(D_x \eta^{2}_{T_{1g}}\right)^{*} - D_y \eta_{A_{1g}} \left(D_z \eta^{3}_{T_{1g}}\right)^{*} + D_z \eta_{A_{1g}} \left(D_y \eta^{3}_{T_{1g}}\right)^{*} + \text{c.c.} \Big\},\end{aligned} \tag{23}$$

$$\begin{aligned}\mathcal{L}^{\nabla}_{A_{1g},T_{2g}} = a_{A_{1g}T_{2g}} \Big\{ & D_x \eta_{A_{1g}} \left(D_y \eta^{1}_{T_{2g}}\right)^{*} + D_y \eta_{A_{1g}} \left(D_x \eta^{1}_{T_{2g}}\right)^{*} + D_x \eta_{A_{1g}} \left(D_z \eta^{2}_{T_{2g}}\right)^{*} \\ & + D_z \eta_{A_{1g}} \left(D_x \eta^{2}_{T_{2g}}\right)^{*} + D_y \eta_{A_{1g}} \left(D_z \eta^{3}_{T_{2g}}\right)^{*} + D_z \eta_{A_{1g}} \left(D_y \eta^{3}_{T_{2g}}\right)^{*} + \text{c.c.} \Big\},\end{aligned} \tag{24}$$

and for the uniform parts $\mathcal{L}^{u}_{A_{1g}\Gamma}$, we use

$$\begin{aligned}\mathcal{L}^{u}_{A_{1g}\Gamma} = {} & c^{1}_{A_{1g}\Gamma} \left|\eta_{A_{1g}}\right|^2 \sum_{i=1}^{d_\Gamma} \left|\eta^{i}_{\Gamma}\right|^2 \\ & + c^{2}_{A_{1g}\Gamma} \left(\eta^{2}_{A_{1g}} \sum_{i=1}^{d_\Gamma} \left(\eta^{i*}_{\Gamma}\right)^2 + \eta^{*2}_{A_{1g}} \sum_{i=1}^{d_\Gamma} \left(\eta^{i}_{\Gamma}\right)^2 \right),\end{aligned} \tag{25}$$

where d_Γ is the dimension of the Γ irrep. When $\Gamma = T_{1u}$, there are no other invariants quartic in OPs. In particular, there are no invariants cubic in $\eta_{T_{1u}}$ and linear in $\eta_{A_{1g}}$ since the inversion symmetry requires an even number of ungerade irreps entering the invariant. When Γ is gerade, there are invariants cubic in η_Γ and linear in $\eta_{A_{1g}}$. However, we do not include them here, as they are of higher order in η_Γ. The rest of the terms entering into Eq. (18) are given in Appendix B.

We further generalize this static Lagrangian model to a time-dependent GL theory. For s-wave superconductors, the simplest TDGL model is obtained by extending the static GL equations to [58]

$$\Gamma_s D_t \eta_s = -\frac{\delta F}{\delta \eta^{*}_{s}}, \tag{26}$$

where $F = \int d^d x \mathcal{L}_{st}$ is the free energy, $D_t = \partial_t + i2e/\hbar \cdot \phi$ is a covariant time derivative, in which ϕ is the electric potential, and Γ_s is the relaxation coefficient. It is microscopically justified for gapless superconductors close to T_c. A generalized TDGL model was derived microscopically for dirty gapped s-wave superconductors near T_c [59,60]. Equation (26) can be obtained by introducing the Rayleigh functional [61]

$$R = \int d^d r \Gamma_s |D_t \eta_s|^2. \tag{27}$$

We do not derive the TDGL model, corresponding to the static Lagrangian in Eq. (18), microscopically. Instead, we write the most general quadratic, gauge-invariant Rayleigh functional:

$$\begin{aligned}R = {} & \int d^d r \sum_{\mu \in \Gamma_r} \sum_{\substack{i,j=1 \\ i \neq j}}^{d_\mu} \Gamma^{ij}_{\nu} \left(D_t \eta^{i}_{\nu}\right)^{*} \left(D_t \eta^{j}_{\nu}\right) \\ & + \int d^d r \sum_{\substack{\mu,\nu \in \Gamma_r \\ \mu \neq \nu}} \sum_{i=1}^{d_\mu} \sum_{j=1}^{d_\nu} \Gamma^{ij}_{\mu\nu} \left(D_t \eta^{i}_{\mu}\right)^{*} \left(D_t \eta^{j}_{\nu}\right).\end{aligned} \tag{28}$$

To preserve rotational invariance of the time-derivative terms, we have to set $\Gamma^{ij}_{\mu\nu} = 0$ and $\Gamma^{ij}_{\nu} = \Gamma_\nu \delta_{ij}$.

IV. TDGL EQUATIONS

A. Equations of motion

The equations of motion are given by

$$\frac{\delta \mathcal{L}}{\delta \eta^{i*}_{\nu}} - \partial_j \frac{\delta \mathcal{L}}{\delta\left(\partial_j \eta^{i*}_{\nu}\right)} + \frac{\delta R}{\delta\left(\partial_t \eta^{i*}_{\nu}\right)} = 0. \tag{29}$$

We explicitly write these equations in dimensionless units. The dimensionless coordinate, time, vector potential, and current are

$$\boldsymbol{r}' = \boldsymbol{r}/\xi, t' = t/\tau_0, \boldsymbol{A}' = \boldsymbol{A}/A_0, \boldsymbol{j}' = \boldsymbol{j}/j_0, \phi' = \phi/\phi_0, \tag{30}$$

where ξ is the coherence length of the pure s-wave uniform SC, $\tau_0 = \mu_0 \sigma \lambda^2$ is the magnetic diffusion time over the London penetration depth λ in the s-wave SC, where μ_0 is the vacuum permeability, σ is the normal conductivity, λ is the magnetic penetration depth of the pure s-wave SC, $A_0 = \xi B_{c2}$, where $B_{c2} = \Phi_0/(2\pi\xi^2)$ is the upper critical magnetic field of the pure s-wave SC, $j_0 = \xi B_{c2}/(\mu_0 \lambda^2)$, and $\phi_0 = \xi j_0/\sigma$. The dimensionless GL parameters are

$$\begin{aligned}& \Gamma'_\nu = \frac{\Gamma_\nu}{\tau_0(-r_{A_{1g}})}, \quad r'_{\Gamma_\nu} = \frac{r_{\Gamma_\nu}}{r_{A_{1g}}}, \quad b^{i}_{\Gamma_\nu}{}' = \frac{b_{\Gamma_\nu}}{b_{A_{1g}}}, \\ & a^{i}_{\Gamma_\nu}{}' = \frac{a_{\Gamma_\nu}}{\xi^2(-r_{A_{1g}})}, \quad a'_{T_{1u}\Gamma_\nu} = \frac{a_{T_{1u}\Gamma_\nu}}{\xi(-r_{A_{1g}})}, \\ & a'_{\substack{\Gamma_\mu\Gamma_\nu \\ \mu \neq T_{1u}}} = \frac{a_{\Gamma_\mu\Gamma_\nu}}{\xi^2(-r_{A_{1g}})}, \quad c^{i}_{A_{1g}\Gamma_\nu}{}' = \frac{c_{A_{1g}\Gamma_\nu}}{b_{A_{1g}}},\end{aligned} \tag{31}$$

and the covariant derivatives in the dimensionless units are

$$D_i' = \partial_i' - iA_i',\ D_t' = \partial_t' + i\phi'. \tag{32}$$

In the following, writing the TDGL equations in dimensionless form, we omit the prime sign ($'$) in dimensionless quantities and the GL parameters. For a thin-film case, for which we assume that dependence on the z coordinate is very weak and derivatives with respect to the z coordinate can be neglected, these equations take the form

$$\begin{aligned}\Gamma_{A_{1g}} D_t \eta_{A_{1g}} = {} & r_{A_{1g}}\,\eta_{A_{1g}} + a_{A_{1g}} \sum_i D_i^2 \eta_{A_{1g}} - b_{A_{1g}} \left|\eta_{A_{1g}}\right|^2 \eta_{A_{1g}} + 2\, a_{A_{1g},T_{1u}} \left(- \sum_i D_i\, \eta_{T_{1u}}^i \right) \\ & + \frac{1}{2}\, a_{A_{1g},E_g} \left(D_x^2 \eta_{E_g}^1 - D_x^2 \eta_{E_g}^2 - D_y^2 \eta_{E_g}^1 - D_y^2 \eta_{E_g}^2 \right) \\ & + a_{A_{1g},T_{1g}} \left(- D_x D_y\, \eta_{T_{1g}}^1 + D_y D_x\, \eta_{T_{1g}}^1 \right) + a_{A_{1g},T_{2g}} \left(D_x D_y\, \eta_{T_{2g}}^1 + D_y D_x\, \eta_{T_{2g}}^1 \right) \\ & - {\sum_{\Gamma\in\Gamma_r}}' c_{A_{1g}\Gamma}^1 \sum_{i=1}^{d_\Gamma} \left|\eta_\Gamma^i\right|^2 \eta_{A_{1g}} - {\sum_{\Gamma\in\Gamma_r}}' c_{A_{1g}\Gamma}^2 \sum_{i=1}^{d_\Gamma} \left(\eta_\Gamma^i\right)^2 \eta_{A_{1g}}^* \end{aligned} \tag{33}$$

for the s-wave OP, where $r_{A_{1g}} = 1$, $a_{A_{1g}} = 1$, and $b_{A_{1g}} = 1$,

$$\begin{aligned}\Gamma_{T_{1u}} D_t \eta_{T_{1u}}^1 = {} & r_{T_{1u}}\,\eta_{T_{1u}}^1 + a_{T_{1u}}^1 D_x^2 \eta_{T_{1u}}^1 + a_{T_{1u}}^2 D_y^2 \eta_{T_{1u}}^1 + a_{T_{1u}}^3 D_x D_y\, \eta_{T_{1u}}^2 + a_{T_{1u}}^4 D_y D_x\, \eta_{T_{1u}}^2 \\ & - 2b_{T_{1u}}^1 \left(\sum_{i=1}^3 \left|\eta_{T_{1u}}^i\right|^2 \right) \eta_{T_{1u}}^1 - 2b_{T_{1u}}^2 \left(\sum_{i=1}^3 \left(\eta_{T_{1u}}^i\right)^2 \right) \eta_{T_{1u}}^{1*} - b_{T_{1u}}^3 \left(\left|\eta_{T_{1u}}^2\right|^2 + \left|\eta_{T_{1u}}^3\right|^2 \right) \eta_{T_{1u}}^1 \\ & + 2a_{A_{1g}T_{1u}} D_x \eta_{A_{1g}} + a_{T_{1u}E_g} \left(D_x \eta_{E_g}^1 - D_x \eta_{E_g}^2 \right) + 2a_{T_{1u}T_{1g}} D_y \eta_{T_{1g}}^1 - 2a_{T_{1u}T_{2g}} D_y \eta_{T_{2g}}^1 \\ & - c_{A_{1g}T_{1u}}^1 \left|\eta_{A_{1g}}\right|^2 \eta_{T_{1u}}^1 - c_{A_{1g}T_{1u}}^2 \left(\eta_{A_{1g}}\right)^2 \eta_{T_{1u}}^{1*}, \end{aligned} \tag{34}$$

$$\begin{aligned}\Gamma_{T_{1u}} D_t \eta_{T_{1u}}^2 = {} & r_{T_{1u}}\,\eta_{T_{1u}}^2 + a_{T_{1u}}^1 D_y^2 \eta_{T_{1u}}^2 + a_{T_{1u}}^2 D_x^2 \eta_{T_{1u}}^2 + a_{T_{1u}}^3 D_y D_x\, \eta_{T_{1u}}^1 + a_{T_{1u}}^4 D_x D_y\, \eta_{T_{1u}}^1 \\ & - 2b_{T_{1u}}^1 \left(\sum_{i=1}^3 \left|\eta_{T_{1u}}^i\right|^2 \right) \eta_{T_{1u}}^2 - 2b_{T_{1u}}^2 \left(\sum_{i=1}^3 \left(\eta_{T_{1u}}^i\right)^2 \right) \eta_{T_{1u}}^{2*} - b_{T_{1u}}^3 \left(\left|\eta_{T_{1u}}^1\right|^2 + \left|\eta_{T_{1u}}^3\right|^2 \right) \eta_{T_{1u}}^2 \\ & + 2a_{A_{1g}T_{1u}} D_y \eta_{A_{1g}} + a_{T_{1u}E_g} \left(- D_y \eta_{E_g}^1 - D_y \eta_{E_g}^2 \right) - 2a_{T_{1u}T_{1g}} D_x \eta_{T_{1g}}^1 - 2a_{T_{1u}T_{2g}} D_x \eta_{T_{2g}}^1 \\ & - c_{A_{1g}T_{1u}}^1 \left|\eta_{A_{1g}}\right|^2 \eta_{T_{1u}}^2 - c_{A_{1g}T_{1u}}^2 \left(\eta_{A_{1g}}\right)^2 \eta_{T_{1u}}^{2*}, \end{aligned} \tag{35}$$

$$\begin{aligned}\Gamma_{T_{1u}} D_t \eta_{T_{1u}}^3 = {} & r_{T_{1u}}\,\eta_{T_{1u}}^3 + a_{T_{1u}}^2 \left(D_x^2 + D_y^2 \right) \eta_{T_{1u}}^3 \\ & - 2b_{T_{1u}}^1 \left(\sum_{i=1}^3 \left|\eta_{T_{1u}}^i\right|^2 \right) \eta_{T_{1u}}^3 - 2b_{T_{1u}}^2 \left(\sum_{i=1}^3 \left(\eta_{T_{1u}}^i\right)^2 \right) \eta_{T_{1u}}^{3*} - b_{T_{1u}}^3 \left(\left|\eta_{T_{1u}}^1\right|^2 + \left|\eta_{T_{1u}}^2\right|^2 \right) \eta_{T_{1u}}^3 \\ & + 2a_{T_{1u}T_{1g}} \left(- D_x \eta_{T_{1g}}^2 - D_y \eta_{T_{1g}}^3 \right) + 2a_{T_{1u}T_{2g}} \left(- D_x \eta_{T_{2g}}^2 - D_y \eta_{T_{2g}}^3 \right) \\ & - c_{A_{1g}T_{1u}}^1 \left|\eta_{A_{1g}}\right|^2 \eta_{T_{1u}}^3 - c_{A_{1g}T_{1u}}^2 \left(\eta_{A_{1g}}\right)^2 \eta_{T_{1u}}^{3*} \end{aligned} \tag{36}$$

for the components of the p-wave OP, and

$$\begin{aligned}\Gamma_{E_g} D_t \eta_{E_g}^1 = {} & r_{E_g}\,\eta_{E_g}^1 + a_{E_g}^1 \sum_{i=1}^3 D_i^2 \eta_{E_g}^1 + a_{E_g}^2 \left(- D_x^2 \eta_{E_g}^1 - D_y^2 \eta_{E_g}^1 + \sqrt{3}\, D_x^2 \eta_{E_g}^2 - \sqrt{3}\, D_y^2 \eta_{E_g}^2 \right) \\ & - 2b_{E_g}^1 \left(\sum_{i=1}^2 \left|\eta_{E_g}^i\right|^2 \right) \eta_{E_g}^1 - 2b_{E_g}^2 \left(\eta_{E_g}^{1*} \eta_{E_g}^2 - \eta_{E_g}^{2*} \eta_{E_g}^1 \right) \eta_{E_g}^2 \\ & + \frac{1}{2}\, a_{A_{1g}E_g} \left(D_x^2 \eta_{A_{1g}} - D_y^2 \eta_{A_{1g}} \right) - a_{T_{1u}E_g} \left(D_x \eta_{T_{1u}}^1 - D_y \eta_{T_{1u}}^2 \right) \\ & + a_{E_gT_{1g}}^1 \left(-\frac{1}{3} D_x D_y \eta_{T_{1g}}^1 - \frac{1}{3} D_y D_x \eta_{T_{1g}}^1 \right) + a_{E_gT_{1g}}^2 \left(-\frac{1}{3} D_x D_y \eta_{T_{1g}}^1 - \frac{1}{3} D_y D_x \eta_{T_{1g}}^1 \right) \\ & + a_{E_gT_{2g}}^1 \left(\frac{1}{3} D_x D_y \eta_{T_{2g}}^1 - \frac{1}{3} D_y D_x \eta_{T_{2g}}^1 \right) + a_{E_gT_{2g}}^2 \left(-\frac{1}{3} D_x D_y \eta_{T_{2g}}^1 + \frac{1}{3} D_y D_x \eta_{T_{2g}}^1 \right) \\ & - c_{A_{1g}E_g}^1 \left|\eta_{A_{1g}}\right|^2 \eta_{E_g}^1 - c_{A_{1g}E_g}^2 \left(\eta_{A_{1g}}\right)^2 \eta_{E_g}^{1*}, \end{aligned} \tag{37}$$

$$\begin{aligned}\Gamma_{E_g} D_t \eta^2_{E_g} &= r_{E_g}\,\eta^2_{E_g} + a^1_{E_g}\sum_{i=1}^{3} D_i^2 \eta^2_{E_g} + a^2_{E_g}\big(D_x^2\eta^2_{E_g} + D_y^2\eta^2_{E_g} + \sqrt{3}\,D_x^2\eta^1_{E_g} - \sqrt{3}\,D_y^2\eta^1_{E_g}\big)\\ &- 2b^1_{E_g}\left(\sum_{i=1}^{2}\left|\eta^i_{E_g}\right|^2\right)\eta^2_{E_g} + 2b^2_{E_g}\big(\eta^{1*}_{E_g}\eta^2_{E_g} - \eta^{2*}_{E_g}\eta^1_{E_g}\big)\eta^1_{E_g}\\ &+ \frac{1}{2}\,a_{A_{1g}E_g}\big(-D_x^2\eta_{A_{1g}} - D_y^2\eta_{A_{1g}}\big) - a_{T_{1u}E_g}\big(-D_x\eta^1_{T_{1u}} - D_y\eta^2_{T_{1u}}\big)\\ &+ a^1_{E_gT_{1g}}\big(D_xD_y\,\eta^1_{T_{1g}} - D_yD_x\,\eta^1_{T_{1g}}\big) + a^2_{E_gT_{1g}}\big(-D_xD_y\,\eta^1_{T_{1g}} + D_yD_x\,\eta^1_{T_{1g}}\big)\\ &+ a^1_{E_gT_{2g}}\big(-D_xD_y\,\eta^1_{T_{2g}} - D_yD_x\,\eta^1_{T_{2g}}\big) + a^2_{E_gT_{2g}}\big(-D_xD_y\,\eta^1_{T_{2g}} - D_yD_x\,\eta^1_{T_{2g}}\big)\\ &- c^1_{A_{1g}E_g}\left|\eta_{A_{1g}}\right|^2\eta^2_{E_g} - c^2_{A_{1g}E_g}\big(\eta_{A_{1g}}\big)^2\eta^{2*}_{E_g}\end{aligned} \tag{38}$$

for the E_g ($d_{x^2-y^2}$ and d_{z^2}) components of the d-wave OP. We write the rest of the TDGL equations in Appendix C.

B. Current

The variation of Eq. (18) with respect to the vector potential yields the expression for the superconducting current. We compactly write terms in the Lagrangian density corresponding to the singlet-to-singlet and triplet-to-triplet couplings as

$$\mathcal{L}_{\mu\nu} = Q^{\alpha\beta}_{\mu\nu,ij}\big(D_i\eta^\alpha_\mu\big)^* D_j\eta^\beta_\nu, \text{ with } Q^{\alpha\beta}_{\mu\nu,ij} = Q^{\beta\alpha}_{\nu\mu,ji} \tag{39}$$

and to the triplet-to-singlet couplings as

$$\mathcal{L}_{T_{1u}\nu} = P^{\alpha\beta}_{\nu,i}\big[\big(D_i\eta^\alpha_{T_{1u}}\big)^*\eta^\beta_\nu - \eta^{\alpha*}_{T_{1u}}D_i\eta^\beta_\nu + \text{c.c.}\big]. \tag{40}$$

The values for $Q^{\alpha\beta}_{\mu\nu,ij}$ and $P^{\alpha\beta}_{\nu,i}$ are given in Appendix D. For the SC current density, we find

$$\boldsymbol{j}_{si} = \frac{4e}{\hbar}\mathrm{Im}Q^{\alpha\beta}_{\mu\nu,ij}\eta^{\alpha*}_\mu D_j\eta^\beta_\nu - \frac{4e}{\hbar}\mathrm{Im}P^{\beta\alpha}_{\nu,i}\eta^{\alpha*}_\nu\eta^\beta_{T_{1u}}. \tag{41}$$

To find the full current, we add the normal component $\boldsymbol{j_n}$:

$$\begin{aligned}\boldsymbol{j} &= \boldsymbol{j_s} + \boldsymbol{j_n}, \quad \text{where}\\ \boldsymbol{j_n} &= \sigma\boldsymbol{E} = -\sigma\left(\nabla\phi + \frac{\partial\boldsymbol{A}}{\partial t}\right).\end{aligned} \tag{42}$$

The electric potential ϕ is then found from the continuity equation

$$\nabla\cdot\boldsymbol{j} = 0, \tag{43}$$

in which the charge-neutrality condition $\partial\rho/\partial t \approx 0$, where ρ is the charge density, is assumed. This standard assumption in TDGL theory is valid because the charge-density fluctuations relax on the plasma-frequency timescale, which is much shorter than the characteristic timescales governing the superconducting order-parameter dynamics. In the dimensionless (primed) units, this yields

$$\nabla^{2'}\phi' = \nabla'\cdot\boldsymbol{j_s}' - \frac{\partial(\nabla'\cdot\boldsymbol{A}')}{\partial t'}. \tag{44}$$

In the dimensionless units, the expression for current is the same as in Eq. (41), except for the absence of the $4e/\hbar$ coefficients, and the expressions for dimensionless $Q^{\alpha\beta'}_{\mu\nu,ij}$ are the same as $Q^{\alpha\beta}_{\mu\nu,ij}$ with the dimensional parameters being substituted with the corresponding dimensionless (primed) ones.

C. Boundary conditions

The system of the TDGL equations (33)–(38) and (C1)–(C6) and Eq. (44) has to be augmented with appropriate boundary conditions, which can be found by requiring the surface term, arising as the result of the variation of the free energy with respect to η^*_ν, to be equal to zero. Generally, depending on the type of the material at the interface with the SC, there is also a surface term contribution to the free energy [62], i.e., $F = \int d^dx\mathcal{L}_{st} + F_{\text{surf}}$. We assume $F_{\text{surf}} = 0$ here, which is the case for a boundary with an insulator [62–65]. Then the boundary conditions take the form

$$\begin{aligned}n_i\big(Q^{\alpha\beta}_{\mu\nu,ij}D_j\eta^\beta_\nu - P^{\beta\alpha}_{\nu,i}\eta^\beta_{T_{1u}}\big) &= 0,\\ n_iP^{\alpha\beta}_{\nu,i}\eta^\beta_\nu &= 0,\end{aligned} \tag{45}$$

where n_i are the components of the normal to the interface unit vector $\boldsymbol{n}$. Note that these two equations imply that the normal to the interface components of both the sum of the singlet-to-singlet and triplet-to-triplet [the first term on the right-hand side of Eq. (41)] and the triplet-to-singlet [the second term on the right-hand side of Eq. (41)] contributions to the SC current vanish separately at the interface.

For numerical simplicity, in the case of a finite-width Gaussian beam, we employ simpler boundary conditions. Expecting that outside the effective area of the beam spot, the induced triplet and singlet components are nearly zero, we use zero boundary conditions for those components:

$$\begin{aligned}\eta^i_{T1u} &= 0, \quad i = 1\ldots3\\ \eta^i_{Eg} &= 0, \quad i = 1,2\\ \eta^i_{T1g} &= 0, \quad i = 1\ldots3\\ \eta^i_{T2g} &= 0, \quad i = 1\ldots3\end{aligned} \tag{46}$$

and the usual boundary condition for the s-wave component of the SC current

$$\boldsymbol{n}\cdot\boldsymbol{D}\eta_{A1g} = 0. \tag{47}$$

This simplification agrees with the results of simulations.

The boundary conditions for Eq. (44) are

$$\boldsymbol{n}\cdot\left(\nabla\phi + \frac{\partial\boldsymbol{A}}{\partial t}\right) = 0, \tag{48}$$

TABLE III. Coefficients in the TDGL model used in the simulations that produced data for Fig. 2. The coefficients are chosen to be comparable with each other based on Refs. [57,68], which show that the intracomponent gradient and quartic Ginzburg-Landau coefficients and the corresponding intercomponent coefficients in specific microscopic models of mixed s- and d-wave superconductors are of the same order, as well as on Refs. [21,69], which show that dimensionless coefficient $a_{A_{1g}T_{1u}}$ can be comparable to $a_{A_{1g}}$ and $a^1_{T_{1u}}$ for realistic parameters of a conventional superconductor on a honeycomb lattice with Kane-Mele SOC. We further extend this to the rest of the static coefficients and set $\Gamma_\nu = \Gamma = 1$ for simplicity.

A_{1g}	$\Gamma_{A_{1g}} = 1, r_{A_{1g}} = 1, b_{A_{1g}} = 1, a_{A_{1g}} = 1, a_{A_{1g}T_{1u}} = 1, a_{A_{1g}E_g} = 1, a_{A_{1g}T_{1g}} = 1, a_{A_{1g}T_{2g}} = 1$
T_{1u}	$\Gamma_{T_{1u}} = 1, r_{T_{1u}} = -30; a^1_{T_{1u}} = 1.1, a^2_{T_{1u}} = 1; a^3_{T_{1u}} = 1.2, a^4_{T_{1u}} = 1.1, b^1_{T_{1u}} = 1, b^2_{T_{1u}} = 1, b^3_{T_{1u}} = 1, a_{T_{1u}E_g} = 1, a_{T_{1u}T_{1g}} = 1.2,$ $a_{T_{1u}T_{2g}} = 1, c^1_{A_{1g}T_{1u}} = c^2_{A_{1g}T_{1u}} = 1$
E_g	$\Gamma_{E_g} = 1, r_{E_g} = -40, a^1_{E_g} = 1.05, a^2_{E_g} = 1, b^1_{E_g} = 1, b^2_{E_g} = 1, a^1_{E_gT_{1g}} = 1.1, a^2_{E_gT_{1g}} = 1, a^1_{E_gT_{2g}} = 1.1, a^2_{E_gT_{2g}} = 1.05$ $c^1_{A_{1g}E_g} = c^2_{A_{1g}E_g} = 1$
T_{1g}	$\Gamma_{T_{1g}} = 1, r_{T_{1g}} = -50, a^1_{T_{1g}} = 1, a^2_{T_{1g}} = 1.05, a^3_{T_{1g}} = 1.1, a^4_{T_{1g}} = 0.95, b^1_{T_{1g}} = 1, b^2_{T_{1g}} = 1, b^3_{T_{1g}} = 1, a^1_{T_{1g}T_{2g}} = 1, a^2_{T_{1g}T_{2g}} = 1.1,$ $a^3_{T_{1g}T_{2g}} = 1.2, c^1_{A_{1g}T_{1g}} = c^2_{A_{1g}T_{1g}} = 1$
T_{2g}	$\Gamma_{T_{2g}} = 1, r_{T_{2g}} = -60, a^1_{T_{2g}} = 0.9, a^2_{T_{2g}} = 0.95, a^3_{T_{2g}} = 0.85, a^4_{T_{2g}} = 0.8, b^1_{T_{2g}} = 1, b^2_{T_{2g}} = 1, b^3_{T_{2g}} = 1,$ $c^1_{A_{1g}T_{2g}} = c^2_{A_{1g}T_{2g}} = 1$

which corresponds to zero normal current flowing through the interfaces.

V. RESULTS FOR INFINITELY WIDE UNIFORM AND GAUSSIAN BEAMS

We start by considering a uniform infinitely wide beam. In that case, a natural assumption is that the solution also has to be uniform. Thus, we neglect the spatial derivatives in the TDGL equations (33)–(38) and (C1)–(C6). The numerical solution of the resulting system of ordinary differential equations (ODEs) for the values of the SC OPs with TDGL parameters given in Table III and the incident $\hat{x}$-polarized microwave with dimensionless frequency $\omega = 1$ and amplitude $A_0 = 0.5$ is plotted in Fig. 2 in red curves. The microscopic validity of the TDGL theory is restricted to a narrow temperature interval close to the superconducting transition $|T - T_c| \ll T_c$, together with the requirement that the order parameters and electromagnetic fields vary slowly on the relevant microscopic spatial and temporal scales. In particular, the microscopic validity of the s-wave TDGL equations assumes that $\Gamma_{A_{1g}} \ll \tau_E^{-1}$ [58,60], where τ_E is the inelastic electron-phonon scattering time. For clean systems, $\tau_E^{-1} \sim \frac{k_B T^3}{\hbar \Theta_D^2}$, where Θ_D is the Debye temperature. For low-temperature superconductors such as Nb, $\tau_E^{-1} \sim 10^9 \mathrm{s}^{-1}$; for superconductors like Nb_3Al and MgB_2, τ_E^{-1} could be $\sim 10^{10} \mathrm{s}^{-1}$; and in cuprates τ_E^{-1} could be $\sim 10^{11}\ \mathrm{s}^{-1}$. In dirty superconductors, τ_E^{-1} might be larger [66]. For example, for dirty NbN thin films $\tau_E^{-1} \sim 10^{11}\ \mathrm{s}^{-1}$ has been reported [67]. Thus, the relevant frequencies of the incident EM radiation are in the microwave range. In Ref. [68], a time-dependent GL theory for a mixed s- and d-wave SC with spherically symmetric Fermi surface was derived, which showed that the corresponding gradient and quartic intracomponent GL parameters and intercomponent GL parameters are of the same order. The same is true for the GL theory with mixed s- and d-wave OPs derived from a microscopic model with nearest-neighbor pairing interactions on a square lattice [57]. We assume here that this is true for the rest of the SC components. In this regard, we note that the microscopically derived value in Ref. [21] of the coefficient for the s-to-p coupling, $a_{A_{1g}T_{1u}}$, in a honeycomb lattice with Kane-Mele spin-orbit coupling model is of the same order as the coefficients for the s-to-s, $a_{A_{1g}}$, and p-to-p, a^1_{T1u}, gradient terms in $\mathcal{L}_{A_{1g}}$ and $\mathcal{L}_{T_{1u}}$, respectively [69]. We also set the relaxation coefficients for each SC component to be the same, i.e., $\Gamma_\nu = \Gamma$.

To gain analytical insight, assuming that the change in $\eta_{A_{1g}}$, $\delta\eta_{A_{1g}} = 1 - \eta_{A_{1g}}$, and the induced components are small, we solve approximate decoupled equations, where the $1s$ now stand for the unperturbed value of $\eta_{A_{1g}}$:

$$\Gamma_{A_{1g}} d_t \eta_{A_{1g}} = \left(1 - \eta^2_{A_{1g}}\right) \eta_{A_{1g}} - A_x^2\, \eta_{A_{1g}}, \tag{49}$$

$$\Gamma_{T_{1u}} d_t \eta^1_{T_{1u}} = r_{T_{1u}}\, \eta^1_{T_{1u}} - a^1_{T_{1u}} A_x^2\, \eta^1_{T_{1u}} - 2\, a_{A_{1g}T_{1u}}\, i A_x \cdot 1 - c^1_{A_{1g}T_{1u}}\, \eta^1_{T_{1u}} + c^2_{A_{1g}T_{1u}}\, \eta^{1*}_{T_{1u}}, \tag{50}$$

$$\Gamma_{T_{1u}} d_t \eta^2_{T_{1u}} = r_{T_{1u}}\, \eta^2_{T_{1u}} - a^2_{T_{1u}} A_x^2\, \eta^2_{T_{1u}} - c^1_{A_{1g}T_{1u}}\, \eta^2_{T_{1u}} - c^2_{A_{1g}T_{1u}}\, \eta^{2*}_{T_{1u}}, \tag{51}$$

$$\Gamma_{T_{1u}} d_t \eta^3_{T_{1u}} = r_{T_{1u}}\, \eta^3_{T_{1u}} - a^2_{T_{1u}} A_x^2\, \eta^3_{T_{1u}} - c^1_{A_{1g}T_{1u}}\, \eta^3_{T_{1u}} - c^2_{A_{1g}T_{1u}}\, \eta^{3*}_{T_{1u}}, \tag{52}$$

$$\Gamma_{E_g} d_t \eta^1_{E_g} = r_{E_g}\, \eta^1_{E_g} - \tfrac{1}{2}\, a_{A_{1g}E_g} A_x^2 \cdot 1 - c^1_{A_{1g}E_g}\, \eta^1_{E_g} - c^2_{A_{1g}E_g}\, \eta^{1*}_{E_g}, \tag{53}$$

$$\Gamma_{E_g} d_t \eta^2_{E_g} = r_{E_g}\, \eta^2_{E_g} + \tfrac{1}{2}\, a_{A_{1g}E_g} A_x^2 \cdot 1 - c^1_{A_{1g}E_g}\, \eta^2_{E_g} - c^2_{A_{1g}E_g}\, \eta^{2*}_{E_g}, \tag{54}$$

omitting the ones for $\eta^i_{T_{1g}}$ and $\eta^i_{T_{2g}}$ as these components remain essentially zero for the chosen parameters.

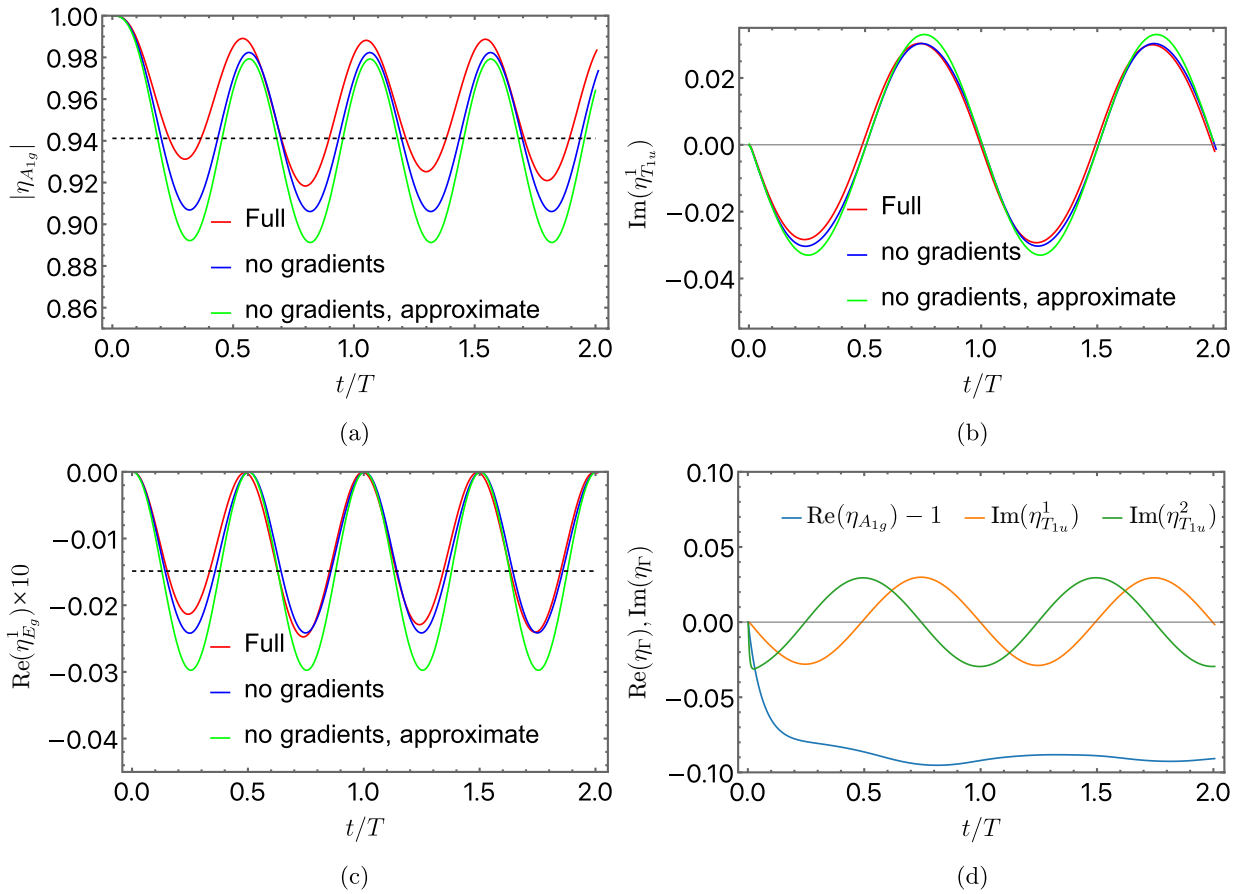


FIG. 2. (a) $|\eta_{A_{1g}}|$ (s wave); (b) $\mathrm{Im}(\eta^1_{T_{1u}})$ (p wave); (c) $\mathrm{Re}(\eta^1_{E_g})$ (d wave). Red and blue curves correspond to the solutions of (33)–(38) and (C1)−(C6) in the cases of Gaussian and uniform linearly polarized beams, respectively. Black curve corresponds to the approximate solution of Eqs. (49)–(54) in the case of a uniform beam. Dashed lines correspond to the approximate average values given by Eq. (57) around which the approximate solutions oscillate. The TDGL parameters are given in Table III, the dimensionless frequency and amplitude of the microwaves are $\omega = 1$ and $A_0 = 0.5$, respectively, the waist of the Gaussian beam is $w_0 = 4\xi$, and the side length of the thin square film is $l = 20\xi$. (d) Time dependence of the values of $\eta_{A_{1g}}$ (s wave), $\eta^1_{T_{1u}}$ (p_y wave in the 2D limit), and $\eta^2_{T_{1u}}$ (p_x wave in the 2D limit) order parameters at the center of the circularly polarized Gaussian beam with waist $w_0 = 4\xi$. The TDGL parameters are given in Table III, the dimensionless frequency and amplitude of the beam are $\omega = 1$ and $A_0 = 0.5$, respectively, the waist of the beam is $w_0 = 4\xi$, and the side length of the thin square film is $l = 20\xi$.

The solutions to Eqs. (49)–(54), linearized in $\delta\eta_{A_{1g}}$, are

$$\eta_{A_{1g}}(t) = 1 - \frac{A_0^2}{\Gamma_{A_{1g}}}\, e^{-\frac{2t}{\Gamma_{A_{1g}}} - \frac{A_0^2 t}{2\Gamma_{A_{1g}}} + \frac{A_0^2 \sin(2\omega t)}{4\omega\Gamma_{A_{1g}}}} \int_0^t \sin^2(\omega t_1)\, e^{\frac{2t_1}{\Gamma_{A_{1g}}} + \frac{A_0^2 t_1}{2\Gamma_{A_{1g}}} - \frac{A_0^2 \sin(2\omega t_1)}{4\omega\Gamma_{A_{1g}}}}\, dt_1,$$

$$\eta^1_{T_{1u}}(t) = -ie^{\Gamma^{-1}_{T_{1u}}(\tilde{r}_{T_{1u}} t - \frac{a_{T_{1u}} A_0^2}{2} t - \frac{a_{T_{1u}} A_0^2}{4} \sin(2\omega t))} \int_0^t 2\, a_{A_{1g}T_{1u}} A_0 \sin(\omega t_1)\, e^{-\Gamma^{-1}_{T_{1u}}(\tilde{r}_{T_{1u}} t_1 - \frac{a_{T_{1u}} A_0^2}{2} t_1 - \frac{a_{T_{1u}} A_0^2}{4} \sin(2\omega t_1))}\, dt_1,$$

$$\eta^2_{T_{1u}}(t) = \eta^3_{T_{1u}}(t) = 0,$$

$$\eta^1_{E_g}(t) = -\eta^2_{E_g}(t) = -\frac{a_{A_{1g}E_g} A_0^2}{4} \frac{4\omega^2\Gamma^2_{E_g} e^{\tilde{r}_{E_g}/\Gamma_{E_g} t} - 4\omega^2\Gamma^2_{E_g} - \tilde{r}^2_{E_g} + \tilde{r}^2_{E_g}\cos(2\omega t) - 2\,\tilde{r}_{E_g}\,\omega\,\Gamma_{E_g}\sin(2\omega t)}{\tilde{r}^3_{E_g} + 4\tilde{r}_{E_g}\omega^2\Gamma^2_{E_g}},$$

$$\eta^1_{T_{1g}}(t) = \eta^2_{T_{1g}}(t) = \eta^3_{T_{1g}}(t) = 0,\ \eta^1_{T_{2g}}(t) = \eta^2_{T_{2g}}(t) = \eta^3_{T_{2g}}(t) = 0, \tag{55}$$

where $\tilde{r}_{T_{1u}} = r_{T_{1u}} - (c_{A_{1g}T_{1u}} - c_{A_{1g}T_{1u}})$ and $\tilde{r}_{E_g} = r_{E_g} - (c_{A_{1g}E_g} + c_{A_{1g}E_g})$.

When $|\frac{A_0^2 t}{2\Gamma_{A_{1g}}} - \frac{A_0^2 \sin(2\omega t)}{4\omega\Gamma_{A_{1g}}}| \ll |\frac{2t}{\Gamma_{A_{1g}}}|$ and $|\frac{a_{T_{1u}}A_0^2}{2}t - \frac{a_{T_{1u}}A_0^2}{4}\sin(2\omega t)| \ll |\tilde{r}_{T_{1u}}t|$, then

$$\eta_{A_{1g}}(t) = 1 - \frac{A_0^2}{4(1+\omega^2\Gamma_{A_{1g}}^2)}\left(\omega^2\Gamma_{A_{1g}}^2 e^{-2t/\Gamma_{A_{1g}}} - \left(1+\omega^2\Gamma_{A_{1g}}^2\right) + \cos(2\omega t) + \omega\Gamma_{A_{1g}}\sin(2\omega t)\right),$$

$$\eta^1_{T_{1u}}(t) = -i\frac{2A_0 a_{A_{1g}T_{1u}}}{\tilde{r}_{T_{1u}}^2 + \omega^2\Gamma_{T_{1u}}^2}\left(\omega\Gamma_{T_{1u}}e^{-\tilde{r}_{T_{1u}}t/\Gamma_{T_{1u}}} + \omega\Gamma_{T_{1u}}\cos(\omega t) + \tilde{r}_{T_{1u}}\sin(\omega t)\right), \tag{56}$$

respectively.

The solutions have the form $\eta_\Gamma(t) = f_\Gamma(t)g_\Gamma(t)$, where $f_\Gamma(t) \to 1$ as t increases and $g_\Gamma(t)$ is a periodic function with period $T = \pi/\omega$. Averaging over the period T in the region where $f_\Gamma(t) \approx 1$, from Eqs. (49)–(54), we find values of η_Γ about which oscillations occur:

$$\eta_{A_{1g}0} = 1 - \frac{A_0^2}{4+A_0^2},$$
$$\eta_{T_{1u}0} = 0,$$
$$\eta^1_{E_g0} = -\eta^2_{E_g0} = \frac{a_{A_{1g}E_g}}{\tilde{r}_{E_g}}A_0^2. \tag{57}$$

One can see that the induced singlet components oscillate around nonzero values due to rectification. The amplitudes of the oscillations $\delta\eta_\Gamma$ can be found approximately as

$$\delta\eta_{A_{1g}0} = \frac{A_0^2}{4(1+\omega^2\Gamma_{A_{1g}}^2)}\left[\cos(\phi_1) + \omega\Gamma_{A_{1g}}\sin(\phi_1)\right], \tag{58}$$

$$\delta\eta^1_{T_{1u}0} = i\frac{2A_0 a_{A_{1g}T_{1u}}}{\tilde{r}_{T_{1u}}^2 + \omega^2\Gamma_{T_{1u}}^2}\left[\omega\Gamma_{T_{1u}}\cos(\phi_2) + \tilde{r}_{T_{1u}}\sin(\phi_2)\right], \tag{59}$$

$$\delta\eta^{1,2}_{E_g0} = -\frac{A_0^2 a_{A_{1g}E_g}}{4(\tilde{r}_{E_g}^2 + 4\omega^2\Gamma_{E_g}^2)}\left[\tilde{r}_{E_g}\cos(\phi_3) - 2\omega\Gamma_{E_g}\sin(\phi_3)\right], \tag{60}$$

where $\phi_1 = \arctan(\omega\Gamma_{A_{1g}})$, $\phi_2 = \arctan(\frac{\tilde{r}_{T_{1u}}}{\omega\Gamma_{T_{1u}}})$, $\phi_3 = \arctan(\frac{2\omega\Gamma_{E_g}}{\tilde{r}_{E_g}})$.

When $\frac{2\omega\Gamma_{T_{1u}}}{\tilde{r}_{T_{1u}}} \ll 1$ and $\frac{2\omega\Gamma_{E_g}}{\tilde{r}_{E_g}} \ll 1$,

$$\delta\eta^1_{T_{1u}0} \approx i\frac{2A_0 a_{A_{1g}T_{1u}}\tilde{r}_{T_{1u}}}{\tilde{r}_{T_{1u}}^2 + \omega^2\Gamma_{T_{1u}}^2}, \quad \text{and}$$

$$\delta\eta^{1,2}_{E_g0} \approx \frac{A_0^2 a_{A_{1g}E_g}\tilde{r}_{E_g}}{4\left(\tilde{r}_{E_g}^2 + 4\omega^2\Gamma_{E_g}^2\right)},$$

respectively.

To assess the effect of spatial derivatives, we simulate the dynamics of a superconducting condensate in a thin square film with a side length $l = 20\xi$ subjected to a linearly polarized Gaussian beam with frequency $\omega/\Gamma^{-1} = 1$ and waist $w_0 = 4\xi$ with the center of the beam incident on the center of the film. As we are not interested in the exact dynamics, we also neglect the change in the scalar potential ϕ. The corresponding vector potential is given by

$$\boldsymbol{A}(\boldsymbol{r}, t) = A_0 e^{-\frac{r^2}{w_0^2}}\sin(\omega t)\hat{\mathbf{x}}. \tag{61}$$

In Figs. 2(a)–2(c), we plot the absolute values of $\eta_{A_{1g}}$, the imaginary part of $\eta^1_{T_{1u}}$, and the real part of $\eta^1_{E_g} \approx -\eta^2_{E_g}$ in the center of the film, the corresponding solutions of Eqs. (33)–(38) and (C1)–(C6) for the uniform beam, and the solutions of the approximate Eqs. (49–(54). The imaginary part of $\eta_{A_{1g}}$, the real part of $\eta^1_{T_{1u}}$, and the imaginary part of $\eta^1_{E_g} \approx -\eta^2_{E_g}$ in the center of the film remain almost zero. The absolute value of $\eta^2_{T_{1u}}$ reaches an appreciable nonzero value away from the center of the film, but still about 20 times smaller than the maximum value of $\eta^1_{T_{1u}}$. The density plots that illustrate this are provided in Appendix E.

In the case of a linearly polarized beam, the average value of the induced triplet component is zero. In the case of a circularly polarized microwave beam, the magnitude of the induced triplet order parameter remains nonzero at all times, even though its individual components oscillate and have zero time-averaged values; see Fig. 2(d) and Eqs. (9)–(12).

In Figs. 3 and 4, we plot the time dependence of the $\mathrm{Re}(\eta_{A_{1g}})$ and $\mathrm{Im}(\eta_{T_{1u}})$ OPs for different values of $r_{T_{1u}}$ ranging from -30 to 0.9 and from -30 to 0, respectively, for the incident uniform linearly polarized microwave with dimensionless $\omega = 1$ and $A_{0x} = 0.5$. For these plots, we use the same values of TDGL parameters as before given in Table III, except that we set $c^2_{A_{1g}T_{1u}} = 0$ for simulations in Fig. 3 to ensure that in the absence of perturbations the ground state is purely s wave for $r_{T_{1u}} > 0$, and for data in Fig. 4, we additionally set $c^1_{A_{1g}T_{1u}} = 0.1$. As can be seen, for values of $|r_{T_{1u}}| \lesssim 1$, a significant amplitude of the $\eta_{T^1_{1u}}$ OP (p_y wave in the 2D limit), up to about 50% of the initial amplitude of the s-wave OP, can be achieved. In such a case, as was pointed out in Ref. [21], if the microwave pulse is suitably tailored, the system might relax into the metastable triplet state after the pulse. However, the description of such a scenario within the limits of validity of the TDGL model requires very close competition between the dominant s-wave and the subdominant p-wave states. As can be seen in Fig. 4, the instantaneous and average values of the $\eta_{A_{1g}}$ OP (s wave) can be increased to values above its equilibrium value. This can be roughly explained as the sum of terms in the right-hand side of the equation of motion for $\eta_{A_{1g}}$ [Eq. (33)],

$$2a_{A_{1g}T_{1u}}i\eta^1_{T_{1u}} + \left(c^1_{A_{1g}T_{1u}}\eta_{A_{1g}} - c^2_{A_{1g}T_{1u}}\eta^*_{A_{1g}}\right)\sum_{i=1}^{3}|\eta^i_{T_{1u}}|^2,$$

effectively counteracts the term $-A_x^2\eta_{A_{1g}}$, which overall decreases the effective temperature.

VI. CONCLUSIONS AND DISCUSSION

We have shown within the generalized GL framework that triplet and non-*s*-wave singlet OPs can be generated in an *s*-wave SC via microwave irradiation. The generation of the triplet component is possible only in the presence of SOC, which enables a linear in spatial derivatives and triplet OP Lifshitz-type invariant. The coefficient in front of this invariant is expected to be approximately linear in the SOC coupling when the SOC is relatively weak [21]. After the minimal substitution procedure, this term brings a linear in the vector potential and *s*-wave OP term into the equation of motion for the triplet OP [see Eqs. (34)–(36)].

For linearly polarized light, the induced triplet OP oscillates around zero average, whereas the induced singlet OPs acquire a nonzero average rectified component. A nonzero magnitude of the induced triplet OP can be maintained at all times by irradiation with a circularly polarized beam; see Fig. 2(d) and Eqs. (9)–(12). In this case, the values of the components of the triplet OP oscillate around zero but do not turn to zero simultaneously.

The presented results further illustrate the utility of stirring the superconducting state with light, the so-called quantum printing (QP) approach [34], in which the quantum state or geometrical structure of light modifies the quantum state of matter. Recently, in the context of superconducting condensates, the QP approach was exemplified by the dynamical induction of vortex-antivortex pairs [24,25] in *s*-wave superconductors, excitations of Higgs modes in superconductors [19,20], and the engineering of a dynamical anomalous Josephson junction [70] in superconducting circuits via structured light.

Practical implementations of the proposed ideas would require a judicious choice of the superconducting material. From the developed theory, it follows that materials with strong SOC and closely competing triplet SC states are favorable for the generation of the triplet OP. Thus, some transition-metal dichalcogenides (TMDs) and heavy-fermion SCs could be good candidates. Given the strict range of microscopic validity of the time-dependent GL theory, this work is primarily a proof of principle that induction of the triplet component in a centrosymmetric singlet SC via microwave radiation is possible. Microscopic calculations are needed to confirm that our findings remain valid at lower temperatures. Potentially, the induction of the triplet OP may open a route to engineering nonequilibrium topologically nontrivial SC states or new ways to control spin-polarized supercurrents.

ACKNOWLEDGMENTS

We gratefully acknowledge helpful discussions with G. Cardoso, S. Gassner, S. Karabatsos, I. Khaymovich, A. Talkachov, and T. T. Yeh. This work was supported by the U.S. Department of Energy, Office of Science, Office of Basic Energy Sciences under Award No. DE-SC-0025580 (A.B. and H.Y.). H.Y. was also supported by the European Research Council under the European Union Seventh Framework ERC-2018-SYG 810451 HERO, the Knut and Alice Wallenberg Foundation KAW 2019.0068. The development of the code is supported by DOE Award No. DE-SC-0025580.

A.B. and H.Y. are responsible for the concept, calculations, and writing of this paper.

DATA AVAILABILITY

Data sets are available from the corresponding author on request. Movies of the simulated dynamics of a SC condensate in a 2D film irradiated by linearly and circularly polarized Gaussian beams and the Python code are available openly in the GeneralizedTDGL_Oh GitHub repository [71].

APPENDIX A: DIRECT PRODUCT TABLE

In this Appendix, we show a direct product table in Table IV for the O_h point group.

APPENDIX B: TERMS IN THE LAGRANGIAN NOT SHOWN IN THE MAIN PART

In this Appendix, we provide the rest of constituent parts of the full static Lagrangian density, Eq. (18), not displayed in the main text:

$$\begin{aligned}\mathcal{L}^{\nabla}_{T_{1u},E_g} = a_{T_{1u}E_g}&\left\{\tfrac{1}{2}\left(D_x\eta^1_{T_{1u}}\right)^*\eta^1_{E_g} - \tfrac{1}{2}\left(D_x\eta^1_{T_{1u}}\right)^*\eta^2_{E_g} - \tfrac{1}{2}\left(D_y\eta^2_{T_{1u}}\right)^*\eta^1_{E_g} - \tfrac{1}{2}\left(D_y\eta^2_{T_{1u}}\right)^*\eta^2_{E_g} + \left(D_z\eta^3_{T_{1u}}\right)^*\eta^2_{E_g} + \text{c.c.}\right\}\\ - a_{T_{1u}E_g}&\left\{\tfrac{1}{2}\,\eta^{1*}_{T_{1u}}D_x\eta^1_{E_g} - \tfrac{1}{2}\,\eta^{1*}_{T_{1u}}D_x\eta^2_{E_g} - \tfrac{1}{2}\,\eta^{2*}_{T_{1u}}D_y\eta^1_{E_g} - \tfrac{1}{2}\,\eta^{2*}_{T_{1u}}D_y\eta^2_{E_g} + \eta^{3*}_{T_{1u}}D_z\eta^2_{E_g} + \text{c.c.}\right\},\end{aligned} \tag{B1}$$

$$\begin{aligned}\mathcal{L}^{\nabla}_{T_{1u},T_{1g}} = a_{T_{1u}T_{1g}}&\left\{-\eta^{1*}_{T_{1u}}D_y\eta^1_{T_{1g}} - \eta^{1*}_{T_{1u}}D_z\eta^2_{T_{1g}} + \eta^{2*}_{T_{1u}}D_x\eta^1_{T_{1g}} - \eta^{2*}_{T_{1u}}D_z\eta^3_{T_{1g}} + \eta^{3*}_{T_{1u}}D_x\eta^2_{T_{1g}} + \eta^{3*}_{T_{1u}}D_y\eta^3_{T_{1g}} + \text{c.c.}\right\}\\ - a_{T_{1u}T_{1g}}&\left\{-\left(D_y\eta^1_{T_{1u}}\right)^*\eta^1_{T_{1g}} - \left(D_z\eta^1_{T_{1u}}\right)^*\eta^2_{T_{1g}} + \left(D_x\eta^2_{T_{1u}}\right)^*\eta^1_{T_{1g}} - \left(D_z\eta^2_{T_{1u}}\right)^*\eta^3_{T_{1g}} + \left(D_x\eta^3_{T_{1u}}\right)^*\eta^2_{T_{1g}} + \left(D_y\eta^3_{T_{1u}}\right)^*\eta^3_{T_{1g}} + \text{c.c.}\right\},\end{aligned} \tag{B2}$$

$$\begin{aligned}\mathcal{L}^{\nabla}_{T_{1u},T_{2g}} = a_{T_{1u}T_{2g}}&\left\{\eta^{1*}_{T_{1u}}D_y\eta^1_{T_{2g}} + \eta^{1*}_{T_{1u}}D_z\eta^2_{T_{2g}} + \eta^{2*}_{T_{1u}}D_x\eta^1_{T_{2g}} + \eta^{2*}_{T_{1u}}D_z\eta^3_{T_{2g}} + \eta^{3*}_{T_{1u}}D_x\eta^2_{T_{2g}} + \eta^{3*}_{T_{1u}}D_y\eta^3_{T_{2g}} + \text{c.c.}\right\}\\ - a_{T_{1u}T_{2g}}&\left\{\left(D_y\eta^1_{T_{1u}}\right)^*\eta^1_{T_{2g}} + \left(D_z\eta^1_{T_{1u}}\right)^*\eta^2_{T_{2g}} + \left(D_x\eta^2_{T_{1u}}\right)^*\eta^1_{T_{2g}} + \left(D_z\eta^2_{T_{1u}}\right)^*\eta^3_{T_{2g}} + \left(D_x\eta^3_{T_{1u}}\right)^*\eta^2_{T_{2g}} + \left(D_y\eta^3_{T_{1u}}\right)^*\eta^3_{T_{2g}} + \text{c.c.}\right\}.\end{aligned} \tag{B3}$$

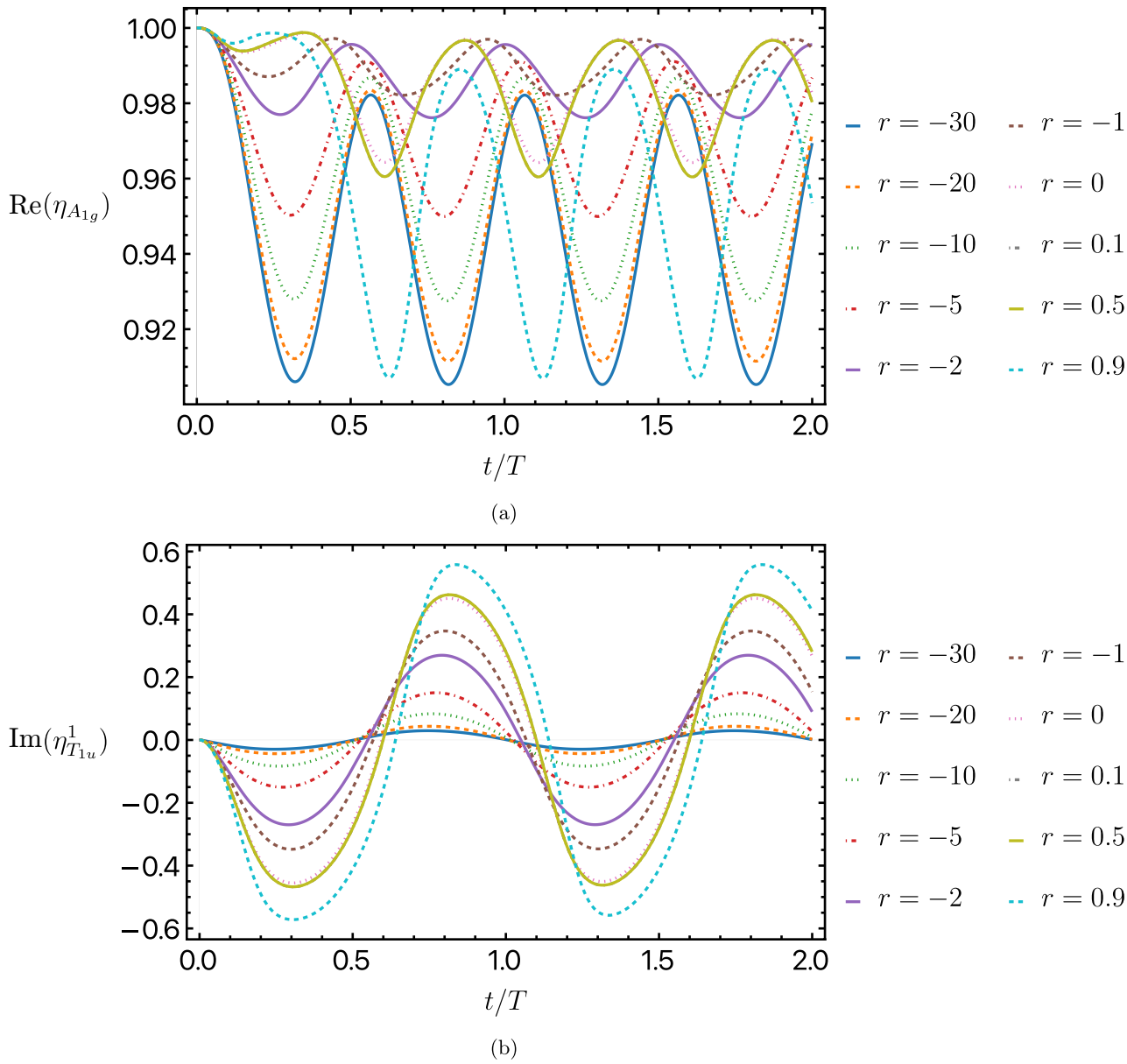


FIG. 3. Time dependence [according to Eqs. (33)–38) and (C1)–(C6)] of $\eta_{A_{1g}}$ (s wave) (a) and $\eta^1_{T_{1u}}$ (p_y wave in the 2D limit). (b) OPs for different values of $r_{T_{1u}}$ ranging from -30 to 0.9, under irradiation by a uniform linearly polarized microwave. The TDGL parameters are given in Table III, except for $c^2_{A_{1g}T_{1u}} = 0$ and values of $r_{T_{1u}} = r$; the dimensionless frequency and amplitude of the microwaves are $\omega = 1$ and $A_0 = 0.5$, respectively. We demonstrate that the induced triplet component can be as large as half of the initial value of the s-wave component.

TABLE IV. Direct product table for the O_h point group (for binary products only).

	A_{1g}	A_{2g}	E_g	T_{1g}	T_{2g}	A_{1u}	A_{2u}	E_u	T_{1u}	T_{2u}
A_{1g}	A_{1g}	A_{2g}	E_g	T_{1g}	T_{2g}	A_{1u}	A_{2u}	E_u	T_{1u}	T_{2u}
A_{2g}	A_{2g}	A_{1g}	E_g	T_{2g}	T_{1g}	A_{2u}	A_{1u}	E_u	T_{2u}	T_{1u}
E_g	E_g	E_g	$A_{1g} \oplus [A_{2g}] \oplus E_g$	$T_{1g} \oplus T_{2g}$	$T_{1g} \oplus T_{2g}$	E_u	E_u	$A_{1u} \oplus A_{2u} \oplus E_u$	$T_{1u} \oplus T_{2u}$	$T_{1u} \oplus T_{2u}$
T_{1g}	T_{1g}	T_{2g}	$T_{1g} \oplus T_{2g}$	$A_{1g} \oplus E_g \oplus [T_{1g}] \oplus T_{2g}$	$A_{2g} \oplus E_g \oplus T_{1g} \oplus T_{2g}$	T_{1u}	T_{2u}	$T_{1u} \oplus T_{2u}$	$A_{1u} \oplus E_u \oplus T_{1u} \oplus T_{2u}$	$A_{2u} \oplus E_u \oplus T_{1u} \oplus T_{2u}$
T_{2g}	T_{2g}	T_{1g}	$T_{1g} \oplus T_{2g}$	$A_{2g} \oplus E_g \oplus T_{1g} \oplus T_{2g}$	$A_{1g} \oplus E_g \oplus [T_{1g}] \oplus T_{2g}$	T_{2u}	T_{1u}	$T_{1u} \oplus T_{2u}$	$A_{2u} \oplus E_u \oplus T_{1u} \oplus T_{2u}$	$A_{1u} \oplus E_u \oplus T_{1u} \oplus T_{2u}$
A_{1u}	A_{1u}	A_{2u}	E_u	T_{1u}	T_{2u}	A_{1g}	A_{2g}	E_g	T_{1g}	T_{2g}
A_{2u}	A_{2u}	A_{1u}	E_u	T_{2u}	T_{1u}	A_{2g}	A_{1g}	E_g	T_{2g}	T_{1g}
E_u	E_u	E_u	$A_{1u} \oplus A_{2u} \oplus E_u$	$T_{1u} \oplus T_{2u}$	$T_{1u} \oplus T_{2u}$	E_g	E_g	$A_{1g} \oplus [A_{2g}] \oplus E_g$	$T_{1g} \oplus T_{2g}$	$T_{1g} \oplus T_{2g}$
T_{1u}	T_{1u}	T_{2u}	$T_{1u} \oplus T_{2u}$	$A_{1u} \oplus E_u \oplus T_{1u} \oplus T_{2u}$	$A_{2u} \oplus E_u \oplus T_{1u} \oplus T_{2u}$	T_{1g}	T_{2g}	$T_{1g} \oplus T_{2g}$	$A_{1g} \oplus E_g \oplus [T_{1g}] \oplus T_{2g}$	$A_{2g} \oplus E_g \oplus T_{1g} \oplus T_{2g}$
T_{2u}	T_{2u}	T_{1u}	$T_{1u} \oplus T_{2u}$	$A_{2u} \oplus E_u \oplus T_{1u} \oplus T_{2u}$	$A_{1u} \oplus E_u \oplus T_{1u} \oplus T_{2u}$	T_{2g}	T_{1g}	$T_{1g} \oplus T_{2g}$	$A_{2g} \oplus E_g \oplus T_{1g} \oplus T_{2g}$	$A_{1g} \oplus E_g \oplus [T_{1g}] \oplus T_{2g}$

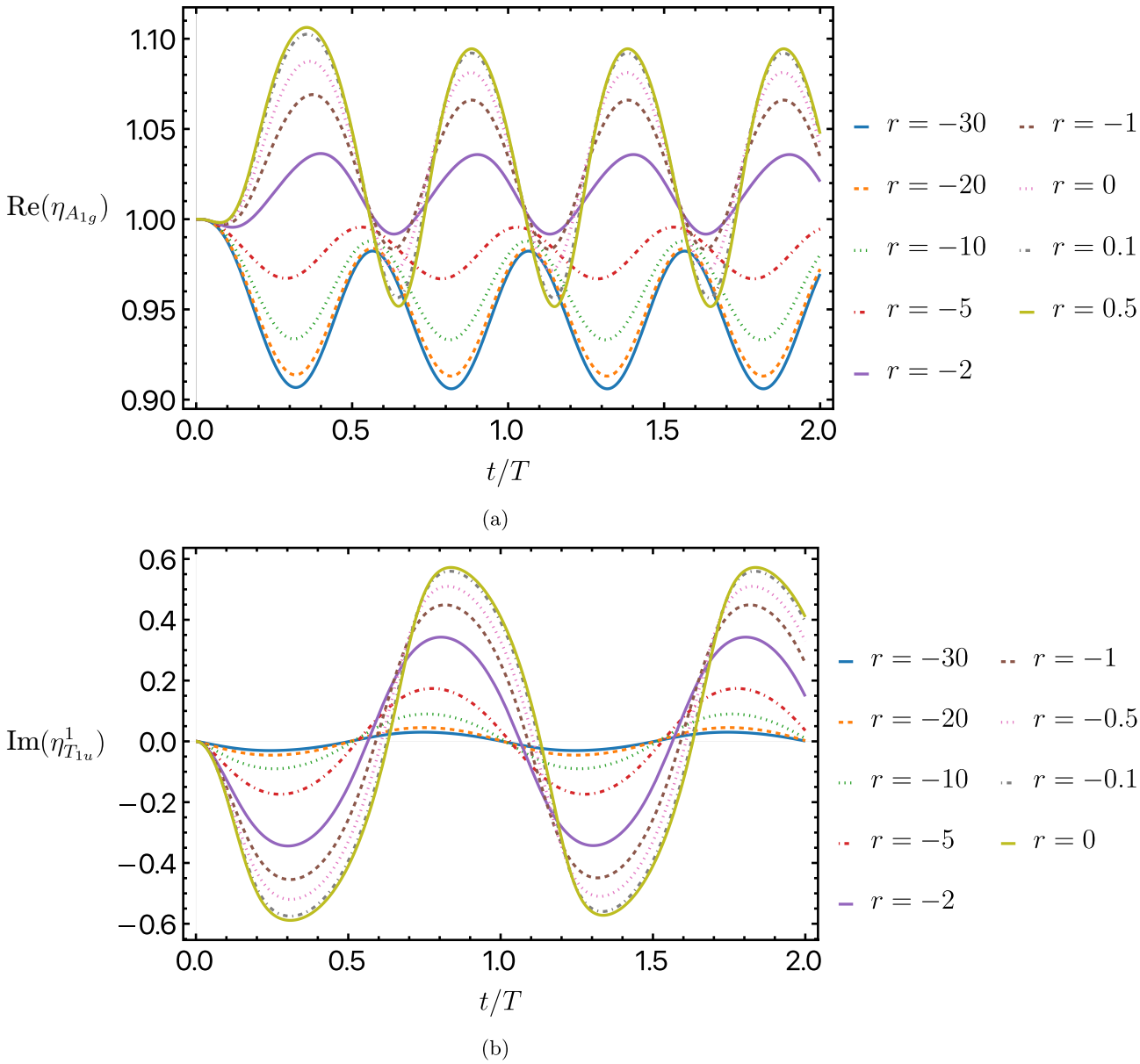


FIG. 4. Time dependence [according to Eqs. (33)–(38) and (C1)–(C6)] of $\eta_{A_{1g}}$ (s wave) (a) and $\eta^1_{T_{1u}}$ (p_y wave in the 2D limit). (b) OPs for different values of $r_{T_{1u}}$ ranging from -30 to 0, under irradiation by a uniform linearly polarized microwave. The TDGL parameters are given in Table III, except for $c^2_{A_{1g}T_{1u}} = 0$, $c^1_{A_{1g}T_{1u}} = 0.1$, and values of $r_{T_{1u}} = r$; the dimensionless frequency and amplitude of the microwaves are $\omega = 1$ and $A_0 = 0.5$, respectively. In this case, the induced triplet component can be as large as about half of the initial value of the s-wave component, and the s-wave can be enhanced transiently above its initial (equilibrium) value.

$$\begin{aligned}\mathcal{L}^{\nabla}_{E_g,T_{1g}} = a^1_{E_gT_{1g}}\Big\{&-\tfrac{1}{3}D_x\eta^1_{E_g}\left(D_y\eta^1_{T_{1g}}\right)^* - \tfrac{1}{3}D_y\eta^1_{E_g}\left(D_x\eta^1_{T_{1g}}\right)^* - \tfrac{2}{3}D_x\eta^1_{E_g}\left(D_z\eta^2_{T_{1g}}\right)^* + \tfrac{1}{3}D_z\eta^1_{E_g}\left(D_x\eta^2_{T_{1g}}\right)^*\\ &+ \tfrac{2}{3}D_y\eta^1_{E_g}\left(D_z\eta^3_{T_{1g}}\right)^* - \tfrac{1}{3}D_z\eta^1_{E_g}\left(D_y\eta^3_{T_{1g}}\right)^* + D_x\eta^2_{E_g}\left(D_y\eta^1_{T_{1g}}\right)^* - D_y\eta^2_{E_g}\left(D_x\eta^1_{T_{1g}}\right)^*\\ &+ D_z\eta^2_{E_g}\left(D_x\eta^2_{T_{1g}}\right)^* + D_z\eta^2_{E_g}\left(D_y\eta^3_{T_{1g}}\right)^* + \text{c.c.}\Big\}\\ + a^2_{E_gT_{1g}}\Big\{&-\tfrac{1}{3}D_x\eta^1_{E_g}\left(D_y\eta^1_{T_{1g}}\right)^* - \tfrac{1}{3}D_y\eta^1_{E_g}\left(D_x\eta^1_{T_{1g}}\right)^* + \tfrac{1}{3}D_x\eta^1_{E_g}\left(D_z\eta^2_{T_{1g}}\right)^* - \tfrac{2}{3}D_z\eta^1_{E_g}\left(D_x\eta^2_{T_{1g}}\right)^*\\ &- \tfrac{1}{3}D_y\eta^1_{E_g}\left(D_z\eta^3_{T_{1g}}\right)^* + \tfrac{2}{3}D_z\eta^1_{E_g}\left(D_y\eta^3_{T_{1g}}\right)^* - D_x\eta^2_{E_g}\left(D_y\eta^1_{T_{1g}}\right)^* + D_y\eta^2_{E_g}\left(D_x\eta^1_{T_{1g}}\right)^*\\ &+ D_x\eta^2_{E_g}\left(D_z\eta^2_{T_{1g}}\right)^* + D_y\eta^2_{E_g}\left(D_z\eta^3_{T_{1g}}\right)^* + \text{c.c.}\Big\},\end{aligned} \tag{B4}$$

$$\begin{aligned}\mathcal{L}^{\nabla}_{E_g,T_{2g}} = a^1_{E_gT_{2g}}\Big\{&\tfrac{1}{3}D_x\eta^1_{E_g}\left(D_y\eta^1_{T_{2g}}\right)^* - \tfrac{1}{3}D_y\eta^1_{E_g}\left(D_x\eta^1_{T_{2g}}\right)^* + \tfrac{2}{3}D_x\eta^1_{E_g}\left(D_z\eta^2_{T_{2g}}\right)^* + \tfrac{1}{3}D_z\eta^1_{E_g}\left(D_x\eta^2_{T_{2g}}\right)^*\\ &- \tfrac{2}{3}D_y\eta^1_{E_g}\left(D_z\eta^3_{T_{2g}}\right)^* - \tfrac{1}{3}D_z\eta^1_{E_g}\left(D_y\eta^3_{T_{2g}}\right)^* - D_x\eta^2_{E_g}\left(D_y\eta^1_{T_{2g}}\right)^* - D_y\eta^2_{E_g}\left(D_x\eta^1_{T_{2g}}\right)^*\\ &+ D_z\eta^2_{E_g}\left(D_x\eta^2_{T_{2g}}\right)^* + D_z\eta^2_{E_g}\left(D_y\eta^3_{T_{2g}}\right)^* + \text{c.c.}\Big\}\\ + a^2_{E_gT_{2g}}\Big\{&-\tfrac{1}{3}D_x\eta^1_{E_g}\left(D_y\eta^1_{T_{2g}}\right)^* + \tfrac{1}{3}D_y\eta^1_{E_g}\left(D_x\eta^1_{T_{2g}}\right)^* + \tfrac{1}{3}D_x\eta^1_{E_g}\left(D_z\eta^2_{T_{2g}}\right)^* + \tfrac{2}{3}D_z\eta^1_{E_g}\left(D_x\eta^2_{T_{2g}}\right)^*\\ &- \tfrac{1}{3}D_y\eta^1_{E_g}\left(D_z\eta^3_{T_{2g}}\right)^* - \tfrac{2}{3}D_z\eta^1_{E_g}\left(D_y\eta^3_{T_{2g}}\right)^* - D_x\eta^2_{E_g}\left(D_y\eta^1_{T_{2g}}\right)^* - D_y\eta^2_{E_g}\left(D_x\eta^1_{T_{2g}}\right)^*\\ &+ D_x\eta^2_{E_g}\left(D_z\eta^2_{T_{2g}}\right)^* + D_y\eta^2_{E_g}\left(D_z\eta^3_{T_{2g}}\right)^* + \text{c.c.}\Big\},\end{aligned} \tag{B5}$$

$$\begin{aligned}\mathcal{L}^{\nabla}_{T_{1g},T_{2g}} = a^1_{T_{1g}T_{2g}}\big\{&- D_x\eta^1_{T_{1g}}\left(D_x\eta^1_{T_{2g}}\right)^* + D_y\eta^1_{T_{1g}}\left(D_y\eta^1_{T_{2g}}\right)^* - D_x\eta^2_{T_{1g}}\left(D_x\eta^2_{T_{2g}}\right)^* + D_z\eta^2_{T_{1g}}\left(D_z\eta^2_{T_{2g}}\right)^*\\ &- D_y\eta^3_{T_{1g}}\left(D_y\eta^3_{T_{2g}}\right)^* + D_z\eta^3_{T_{1g}}\left(D_z\eta^3_{T_{2g}}\right)^* + \text{c.c.}\big\}\\ + a^2_{T_{1g}T_{2g}}\big\{&- D_x\eta^1_{T_{1g}}\left(D_z\eta^3_{T_{2g}}\right)^* + D_z\eta^3_{T_{1g}}\left(D_x\eta^1_{T_{2g}}\right)^* + D_y\eta^1_{T_{1g}}\left(D_z\eta^2_{T_{2g}}\right)^* + D_z\eta^2_{T_{1g}}\left(D_y\eta^1_{T_{2g}}\right)^*\\ &- D_x\eta^2_{T_{1g}}\left(D_y\eta^3_{T_{2g}}\right)^* + D_z\eta^3_{T_{1g}}\left(D_x\eta^1_{T_{2g}}\right)^* + \text{c.c.}\big\}\\ + a^3_{T_{1g}T_{2g}}\big\{&- D_z\eta^1_{T_{1g}}\left(D_x\eta^3_{T_{2g}}\right)^* + D_x\eta^3_{T_{1g}}\left(D_z\eta^1_{T_{2g}}\right)^* + D_z\eta^1_{T_{1g}}\left(D_y\eta^2_{T_{2g}}\right)^* + D_y\eta^2_{T_{1g}}\left(D_z\eta^1_{T_{2g}}\right)^*\\ &- D_y\eta^2_{T_{1g}}\left(D_x\eta^3_{T_{2g}}\right)^* - D_x\eta^3_{T_{1g}}\left(D_y\eta^2_{T_{2g}}\right)^* + \text{c.c.}\big\}.\end{aligned} \tag{B6}$$

APPENDIX C: TDGL EQUATIONS NOT SHOWN IN THE MAIN TEXT

In this Appendix, we write the rest of the TDGL equations not shown in the main text:

$$\begin{aligned}\Gamma_{T_{1g}}D_t\eta^1_{T_{1g}} = {}& r_{T_{1g}}\eta^1_{T_{1g}} + a^1_{T_{1g}}D_x^2\eta^1_{T_{1g}} + a^2_{T_{1g}}D_y^2\eta^1_{T_{1g}} + a^3_{T_{1g}}D_xD_y\,\eta^2_{T_{1g}} + a^4_{T_{1g}}D_yD_x\,\eta^2_{T_{1g}}\\ &- 2b^1_{T_{1g}}\left(\sum_{i=1}^{3}\left|\eta^i_{T_{1g}}\right|^2\right)\eta^1_{T_{1g}} - 2b^2_{T_{1g}}\left(\sum_{i=1}^{3}\left(\eta^i_{T_{1g}}\right)^2\right)\eta^{1*}_{T_{1g}} - b^3_{T_{1g}}\left(\left|\eta^2_{T_{1g}}\right|^2 + \left|\eta^3_{T_{1g}}\right|^2\right)\eta^1_{T_{1g}}\\ &+ a_{A_{1g}T_{1g}}\left(-D_yD_x\,\eta_{A_{1g}} + D_xD_y\,\eta_{A_{1g}}\right) + 2a_{T_{1u}T_{1g}}\left(-D_y\eta^1_{T_{1u}} + D_x\eta^2_{T_{1u}}\right)\\ &+ a^1_{E_gT_{1g}}\left(-\frac{1}{3}D_yD_x\,\eta^1_{E_g} - \frac{1}{3}D_xD_y\,\eta^1_{E_g} + D_yD_x\,\eta^2_{E_g} - D_xD_y\,\eta^2_{E_g}\right)\\ &+ a^2_{E_gT_{1g}}\left(-\frac{1}{3}D_yD_x\,\eta^1_{E_g} - \frac{1}{3}D_xD_y\,\eta^1_{E_g} - D_yD_x\,\eta^2_{E_g} + D_xD_y\,\eta^2_{E_g}\right)\\ &+ a^1_{T_{1g}T_{2g}}\left(-D_x^2\eta^1_{T_{2g}} + D_y^2\eta^1_{T_{2g}}\right) - c^1_{A_{1g}T_{1g}}|\eta_{A_{1g}}|^2\eta^1_{T_{1g}} - c^2_{A_{1g}T_{1g}}\left(\eta_{A_{1g}}\right)^2\eta^{1*}_{T_{1g}},\end{aligned} \tag{C1}$$

$$\begin{aligned}\Gamma_{T_{1g}}D_t\eta^2_{T_{1g}} = {}& r_{T_{1g}}\eta^2_{T_{1g}} + a^1_{T_{1g}}D_y^2\eta^2_{T_{1g}} + a^2_{T_{1g}}D_x^2\eta^2_{T_{1g}} + a^3_{T_{1g}}D_yD_x\,\eta^1_{T_{1g}} + a^4_{T_{1g}}D_xD_y\,\eta^1_{T_{1g}}\\ &- 2b^1_{T_{1g}}\left(\sum_{i=1}^{3}\left|\eta^i_{T_{1g}}\right|^2\right)\eta^2_{T_{1g}} - 2b^2_{T_{1g}}\left(\sum_{i=1}^{3}\left(\eta^i_{T_{1g}}\right)^2\right)\eta^{2*}_{T_{1g}} - b^3_{T_{1g}}\left(\left|\eta^1_{T_{1g}}\right|^2 + \left|\eta^3_{T_{1g}}\right|^2\right)\eta^2_{T_{1g}}\\ &+ 2a_{T_{1u}T_{1g}}D_x\,\eta^3_{T_{1u}} - a^1_{T_{1g}T_{2g}}D_x^2\eta^2_{T_{2g}} - a^2_{T_{1g}T_{2g}}D_xD_y\,\eta^3_{T_{2g}} - a^3_{T_{1g}T_{2g}}D_yD_x\,\eta^3_{T_{2g}}\\ &- c^1_{A_{1g}T_{1g}}|\eta_{A_{1g}}|^2\eta^2_{T_{1g}} - c^2_{A_{1g}T_{1g}}\left(\eta_{A_{1g}}\right)^2\eta^{2*}_{T_{1g}},\end{aligned} \tag{C2}$$

$$\Gamma_{T_{1g}} D_t \eta^3_{T_{1g}} = r_{T_{1g}} \eta^3_{T_{1g}} + a^2_{T_{1g}} \left(D_x^2 \eta^3_{T_{1g}} + D_y^2 \eta^3_{T_{1g}}\right) - 2b^1_{T_{1g}} \left(\sum_{i=1}^{3} \left|\eta^i_{T_{1g}}\right|^2\right) \eta^3_{T_{1g}} - 2b^2_{T_{1g}} \left(\sum_{i=1}^{3} \left(\eta^i_{T_{1g}}\right)^2\right) \eta^{3*}_{T_{1g}}$$
$$- b^3_{T_{1g}} \left(\left|\eta^1_{T_{1g}}\right|^2 + \left|\eta^2_{T_{1g}}\right|^2\right) \eta^3_{T_{1g}} - a^1_{T_{1g}T_{2g}} D_y^2 \eta^3_{T_{2g}} - a^3_{T_{1g}T_{2g}} D_x D_y \eta^2_{T_{2g}} - c^1_{A_{1g}T_{1g}} |\eta_{A_{1g}}|^2 \eta^3_{T_{1g}} - c^2_{A_{1g}T_{1g}} \left(\eta_{A_{1g}}\right)^2 \eta^{3*}_{T_{1g}}, \tag{C3}$$

for the components of the g-wave OP,

$$\begin{aligned}
\Gamma_{T_{2g}} D_t \eta^1_{T_{2g}} = {} & r_{T_{2g}} \eta^1_{T_{2g}} + a^1_{T_{2g}} D_x^2 \eta^1_{T_{2g}} + a^2_{T_{2g}} D_y^2 \eta^1_{T_{2g}} + a^3_{T_{2g}} D_x D_y \eta^2_{T_{2g}} + a^4_{T_{2g}} D_y D_x \eta^2_{T_{2g}} \\
& - 2b^1_{T_{2g}} \left(\sum_{i=1}^{3} \left|\eta^i_{T_{2g}}\right|^2\right) \eta^1_{T_{2g}} - 2b^2_{T_{2g}} \left(\sum_{i=1}^{3} \left(\eta^i_{T_{2g}}\right)^2\right) \eta^{1*}_{T_{2g}} - b^3_{T_{2g}} \left(\left|\eta^2_{T_{2g}}\right|^2 + \left|\eta^3_{T_{2g}}\right|^2\right) \eta^1_{T_{2g}} \\
& + a_{A_{1g}T_{2g}} \left(D_y D_x \eta_{A_{1g}} + D_x D_y \eta_{A_{1g}}\right) + 2a_{T_{1u}T_{2g}} \left(D_y \eta^1_{T_{1u}} + D_x \eta^2_{T_{1u}}\right) \\
& + a^1_{E_gT_{2g}} \left(\frac{1}{3} D_y D_x \eta^1_{E_g} - \frac{1}{3} D_x D_y \eta^1_{E_g} - D_y D_x \eta^2_{E_g} - D_x D_y \eta^2_{E_g}\right) \\
& + a^2_{E_gT_{2g}} \left(-\frac{1}{3} D_y D_x \eta^1_{E_g} + \frac{1}{3} D_x D_y \eta^1_{E_g} - D_y D_x \eta^2_{E_g} - D_x D_y \eta^2_{E_g}\right) \\
& + a^1_{T_{1g}T_{2g}} \left(-D_x^2 \eta^1_{T_{1g}} + D_y^2 \eta^1_{T_{1g}}\right) - c^1_{A_{1g}T_{2g}} |\eta_{A_{1g}}|^2 \eta^1_{T_{2g}} - c^2_{A_{1g}T_{2g}} \left(\eta_{A_{1g}}\right)^2 \eta^{1*}_{T_{2g}},
\end{aligned} \tag{C4}$$

$$\begin{aligned}
\Gamma_{T_{2g}} D_t \eta^2_{T_{2g}} = {} & r_{T_{2g}} \eta^2_{T_{2g}} + a^1_{T_{2g}} D_y^2 \eta^2_{T_{2g}} + a^2_{T_{2g}} D_x^2 \eta^2_{T_{2g}} + a^3_{T_{2g}} D_y D_x \eta^1_{T_{2g}} + a^4_{T_{2g}} D_x D_y \eta^1_{T_{2g}} - 2b^1_{T_{2g}} \left(\sum_{i=1}^{3} \left|\eta^i_{T_{2g}}\right|^2\right) \eta^2_{T_{2g}} \\
& - 2b^2_{T_{2g}} \left(\sum_{i=1}^{3} \left(\eta^i_{T_{2g}}\right)^2\right) \eta^{2*}_{T_{2g}} - b^3_{T_{2g}} \left(\left|\eta^1_{T_{2g}}\right|^2 + \left|\eta^3_{T_{2g}}\right|^2\right) \eta^2_{T_{2g}} + 2a_{T_{1u}T_{2g}} D_x \eta^3_{T_{1u}} - a^1_{T_{1g}T_{2g}} D_x^2 \eta^2_{T_{1g}} - a^3_{T_{1g}T_{2g}} D_y D_x \eta^3_{T_{1g}} \\
& - c^1_{A_{1g}T_{2g}} |\eta_{A_{1g}}|^2 \eta^2_{T_{2g}} - c^2_{A_{1g}T_{2g}} \left(\eta_{A_{1g}}\right)^2 \eta^{2*}_{T_{2g}},
\end{aligned} \tag{C5}$$

$$\Gamma_{T_{2g}} D_t \eta^3_{T_{2g}} = r_{T_{2g}} \eta^3_{T_{2g}} + a^2_{T_{2g}} \left(D_x^2 + D_y^2\right) \eta^3_{T_{2g}} - 2b^1_{T_{2g}} \left(\sum_{i=1}^{3} \left|\eta^i_{T_{2g}}\right|^2\right) \eta^3_{T_{2g}} - 2b^2_{T_{2g}} \left(\sum_{i=1}^{3} \left(\eta^i_{T_{2g}}\right)^2\right) \eta^{3*}_{T_{2g}} - b^3_{T_{2g}} \left(\left|\eta^1_{T_{2g}}\right|^2 + \left|\eta^2_{T_{2g}}\right|^2\right) \eta^3_{T_{2g}}$$
$$- a^1_{T_{1g}T_{2g}} D_y^2 \eta^3_{T_{1g}} - a^2_{T_{1g}T_{2g}} D_y D_x \eta^2_{T_{1g}} - a^3_{T_{1g}T_{2g}} D_x D_y \eta^2_{T_{1g}} - c^1_{A_{1g}T_{2g}} |\eta_{A_{1g}}|^2 \eta^3_{T_{2g}} - c^2_{A_{1g}T_{2g}} \left(\eta_{A_{1g}}\right)^2 \eta^{3*}_{T_{2g}}, \tag{C6}$$

for the T_{2g} components (d_{xy}, d_{xz}, and d_{yz}) of the d-wave OP.

APPENDIX D: COEFFICIENTS FOR THE CONDENSED FORM OF THE LAGRANGIAN

In this Appendix, we provide values for the coefficients $Q^{\alpha\beta}_{\mu\nu,ij}$ and $P^{\alpha\beta}_{\nu,i}$ in Eqs. (39) and (40):

$$\begin{aligned}
& Q^{ii}_{T_{2g}T_{2g},ii} = a^1_{T_{2g}}, \quad Q^{22}_{T_{2g}T_{2g},11} = a^2_{T_{2g}} = Q^{33}_{T_{2g}T_{2g},11} = Q^{11}_{T_{2g}T_{2g},22} = Q^{33}_{T_{2g}T_{2g},22}, \quad Q^{12}_{T_{2g}T_{2g},12} = a^3_{T_{2g}}, \\
& Q^{21}_{T_{2g}T_{2g},12} = a^4_{T_{2g}}, \quad \text{else } Q^{\alpha\beta}_{T_{2g}T_{2g},ij} = 0, \\
& Q^{11}_{T_{1g}T_{2g},11} = -a^1_{T_{1g}T_{2g}} = -Q^{11}_{T_{1g}T_{2g},22} = Q^{22}_{T_{1g}T_{2g},11} = Q^{33}_{T_{1g}T_{2g},22}, \quad Q^{23}_{T_{1g}T_{2g},12} = -a^2_{T_{1g}T_{2g}}, \\
& Q^{23}_{T_{1g}T_{2g},21} = -a^3_{T_{1g}T_{2g}} = Q^{32}_{T_{1g}T_{2g},12}, \quad \text{else } Q^{\alpha\beta}_{T_{1g}T_{2g},ij} = 0, \\
& Q^{ii}_{T_{1g}T_{1g},ii} = a^1_{T_{1g}}, \quad Q^{22}_{T_{1g}T_{1g},11} = a^2_{T_{1g}} = Q^{33}_{T_{1g}T_{1g},11} = Q^{11}_{T_{1g}T_{1g},22} = \quad Q^{33}_{T_{1g}T_{1g},22}, \; Q^{12}_{T_{1g}T_{1g},12} = a^3_{T_{1g}}, \\
& Q^{21}_{T_{1g}T_{1g},12} = a^4_{T_{1g}}, \quad \text{else } Q^{\alpha\beta}_{T_{1g}T_{1g},ij} = 0, \\
& Q^{11}_{E_gT_{2g},12} = \tfrac{1}{3}\left(a^1_{E_gT_{2g}} - a^2_{E_gT_{2g}}\right) = -Q^{11}_{E_gT_{2g},21}, \quad Q^{21}_{E_gT_{2g},12} = -\left(a^1_{E_gT_{2g}} + a^2_{E_gT_{2g}}\right) = Q^{21}_{E_gT_{2g},21}, \quad \text{else } Q^{\alpha\beta}_{E_gT_{2g},ij} = 0, \\
& Q^{11}_{E_gT_{1g},12} = -\tfrac{1}{3}\left(a^1_{E_gT_{1g}} - a^2_{E_gT_{1g}}\right) = Q^{11}_{E_gT_{1g},21}, \quad Q^{21}_{E_gT_{1g},12} = a^1_{E_gT_{1g}} - a^2_{E_gT_{1g}} = -Q^{21}_{E_gT_{1g},21}, \quad \text{else } Q^{\alpha\beta}_{E_gT_{1g},ij} = 0, \\
& Q^{11}_{E_gE_g,11} = a^1_{E_g} - a^2_{E_g} = Q^{11}_{E_gE_g,22}, \quad Q^{22}_{E_gE_g,11} = a^1_{E_g} + a^2_{E_g} = Q^{22}_{E_gE_g,22}, \quad Q^{12}_{E_gE_g,11} = \sqrt{3}\, a^2_{E_g} = Q^{21}_{E_gE_g,11}, \\
& Q^{12}_{E_gE_g,22} = -\sqrt{3}\, a^2_{E_g} = Q^{21}_{E_gE_g,22}, \quad \text{else } Q^{\alpha\beta}_{E_gE_g,ij} = 0, \\
& Q^{11}_{A_{1g}A_{1g},ij} = a_{A_{1g}} \delta_{ij} \delta_{\alpha\beta},
\end{aligned}$$

$$
\begin{aligned}
&Q^{11}_{A_{1g}E_g,11} = \tfrac{1}{2}\, a_{A_{1g}E_g} = -Q^{12}_{A_{1g}E_g,11} = -Q^{11}_{A_{1g}E_g,22} = -Q^{12}_{A_{1g}E_g,22}, \quad \text{else } Q^{\alpha\beta}_{A_{1g}E_g,ij} = 0,\\
&Q^{11}_{A_{1g}T_{2g},12} = a_{A_{1g}T_{2g}} = Q^{11}_{A_{1g}T_{2g},21}, \quad \text{else} \quad Q^{\alpha\beta}_{A_{1g}T_{2g},ij} = 0,\\
&Q^{11}_{A_{1g}T_{1g},12} = -a_{A_{1g}T_{1g}} = -Q^{11}_{A_{1g}T_{1g},21}, \quad \text{else} \quad Q^{\alpha\beta}_{A_{1g}T_{1g},ij} = 0.
\end{aligned} \tag{D1}
$$

$$
\begin{aligned}
&P^{i1}_{A_{1g},i} = a_{A_{1g}T_{1u}}, \quad \text{else } P^{\alpha\beta}_{A_{1g},i} = 0,\\
&P^{11}_{E_g,1} = \tfrac{1}{2}\, a_{T_{1u}E_g} = -P^{12}_{E_g,1} = -P^{21}_{E_g,2} = -P^{22}_{E_g,2}, \quad \text{else } P^{\alpha\beta}_{E_g,i} = 0,\\
&P^{11}_{T_{2g},2} = -a_{T_{1u}T_{2g}} = P^{21}_{T_{2g},1} = P^{32}_{T_{2g},1} = P^{33}_{T_{2g},2}, \quad \text{else } P^{\alpha\beta}_{T_{2g},i} = 0,\\
&P^{11}_{T_{1g},2} = a_{T_{1u}T_{1g}} = -P^{21}_{T_{1g},1} = -P^{32}_{T_{1g},1} = -P^{33}_{T_{1g},2}, \quad \text{else } P^{\alpha\beta}_{T_{1g},i} = 0.
\end{aligned} \tag{D2}
$$

APPENDIX E: DENSITY PLOTS FOR THE TIME EVOLUTION OF OPS

In this Appendix, we provide density plots for the absolute values of the s-wave $\eta_{A_{1g}}$, d-wave $\eta^{1,2}_{E_g}$, and p-wave $\eta^{1,2,3}_{T_{1u}}$ OPs under incident linearly polarized microwave beams at $t/T \approx 0.25$, 0.5, 0.75, and 1, shown in Figs. 5–8, respectively, and under circularly polarized microwave beams at the same times, shown in Figs. 9–12, respectively. They show that the induced subdominant order parameters are localized predominantly within the beam spot and exhibit a nontrivial spatial structure.

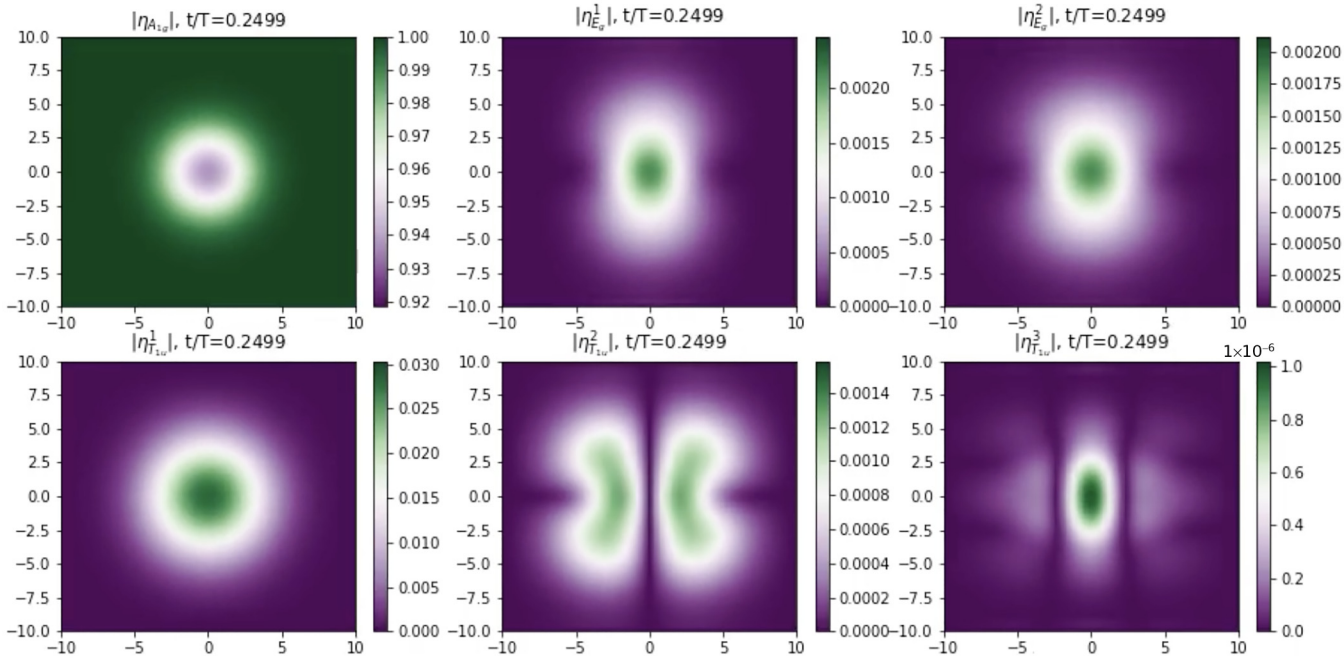


FIG. 5. Density plots for the absolute values of s-wave $\eta_{A_{1g}}$, d-wave $\eta^{1,2}_{Eg}$, and p-wave $\eta^{1,2,3}_{T_{1u}}$ OPs under an incident linearly polarized microwave beam at approximately one quarter of the microwave cycle, $t/T \approx 0.25$, where T is the period of the microwave. Coordinates on the thin film are given in units of ξ.

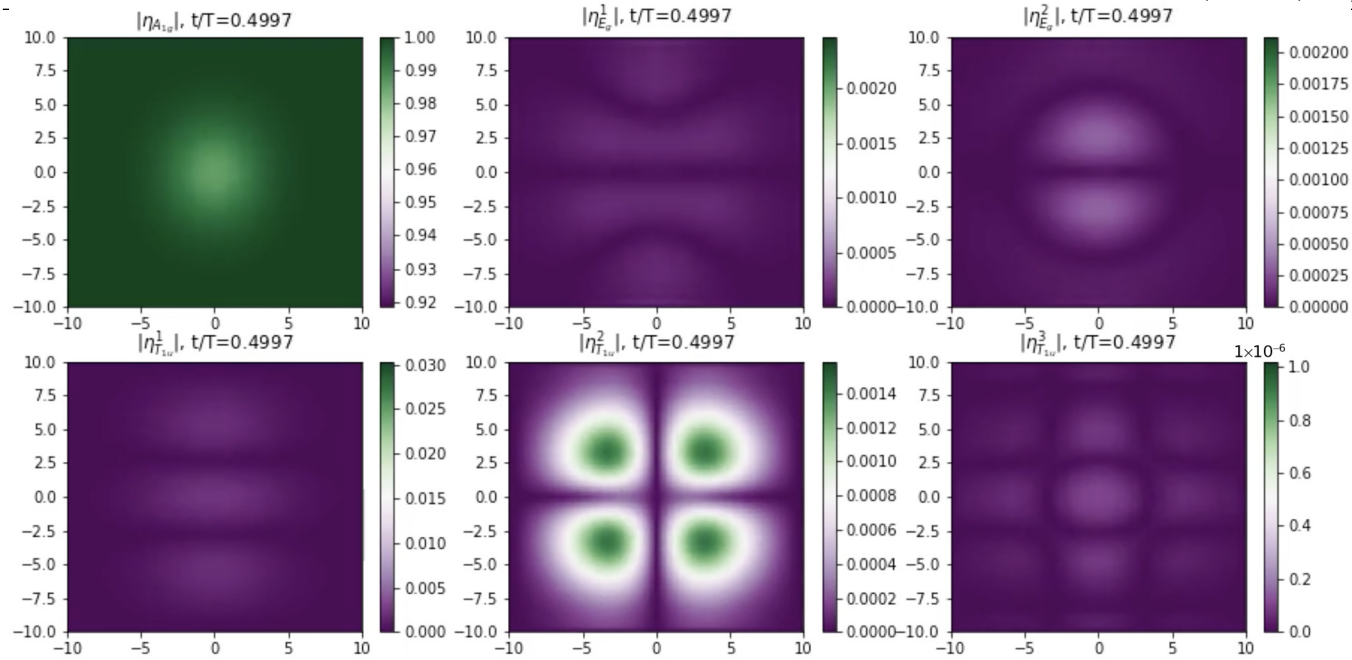


FIG. 6. Density plots for the absolute values of s-wave $\eta_{A_{1g}}$, d-wave $\eta^{1,2}_{Eg}$, and p-wave $\eta^{1,2,3}_{T_{1u}}$ OPs under an incident linearly polarized microwave beam at approximately half of the microwave cycle, $t/T \approx 0.5$, where T is the period of the microwave. Coordinates on the thin film are given in units of ξ.

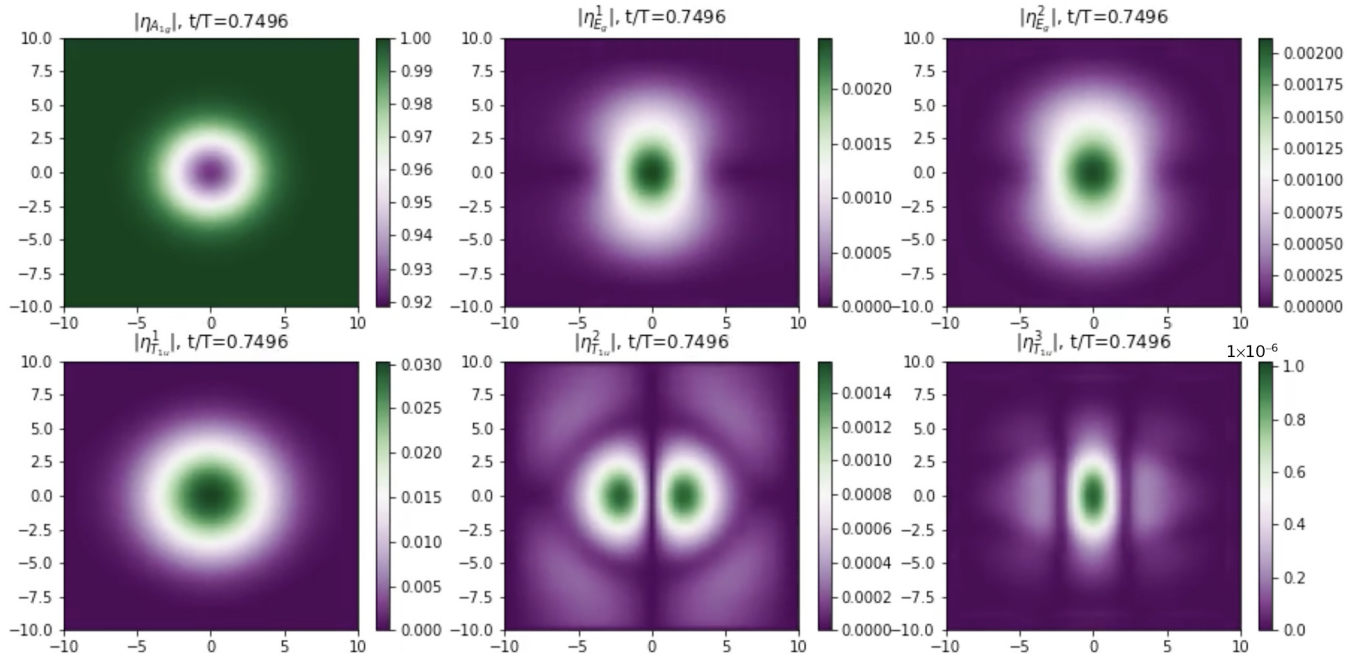


FIG. 7. Density plots for the absolute values of s-wave $\eta_{A_{1g}}$, d-wave $\eta^{1,2}_{Eg}$, and p-wave $\eta^{1,2,3}_{T_{1u}}$ OPs under an incident linearly polarized microwave beam at approximately three quarters of the microwave cycle, $t/T \approx 0.75$, where T is the period of the microwave. Coordinates on the thin film are given in units of ξ.

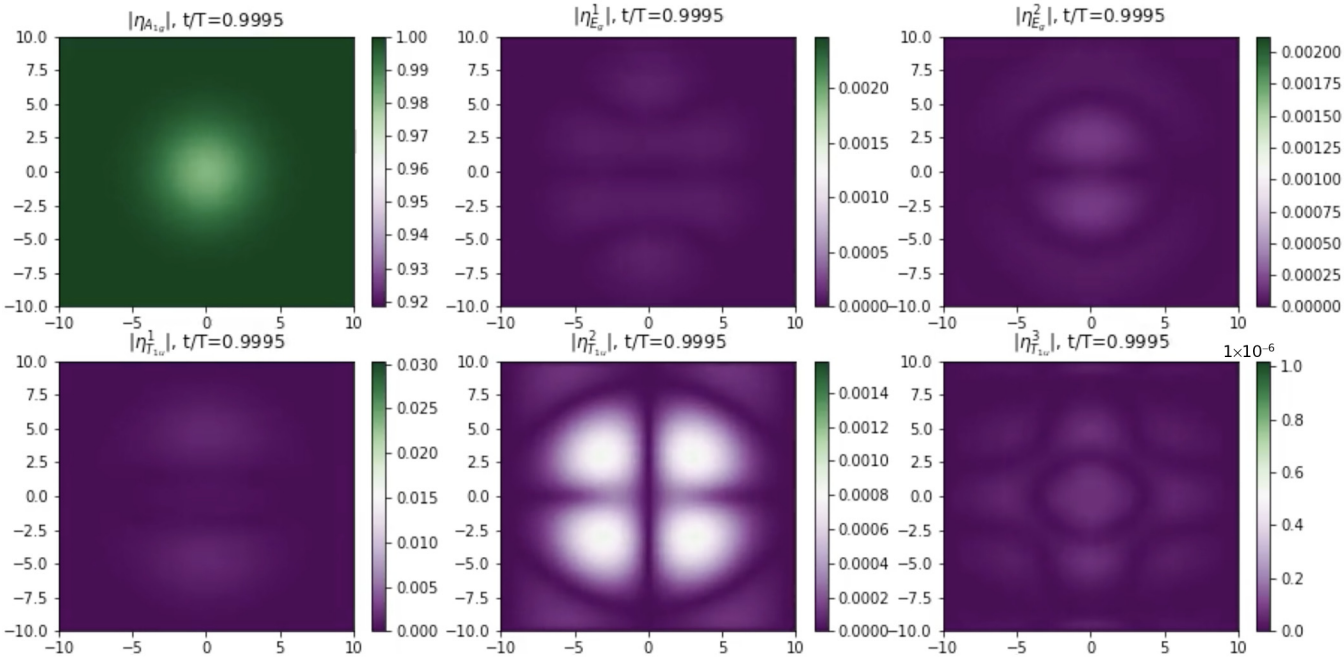


FIG. 8. Density plots for the absolute values of s-wave $\eta_{A_{1g}}$, d-wave $\eta^{1,2}_{Eg}$, and p-wave $\eta^{1,2,3}_{T_{1u}}$ OPs under an incident linearly polarized microwave beam at approximately one full microwave cycle, $t/T \approx 1$, where T is the period of the microwave. Coordinates on the thin film are given in units of ξ.

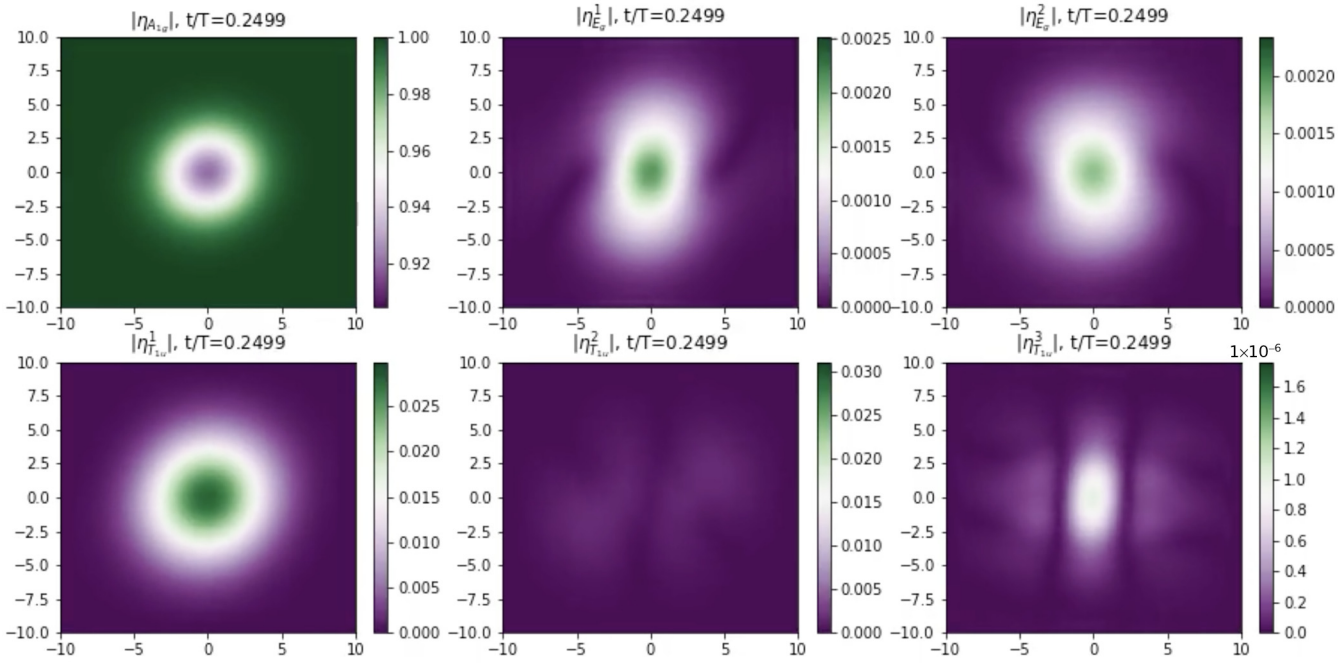


FIG. 9. Density plots for the absolute values of s-wave $\eta_{A_{1g}}$, d-wave $\eta^{1,2}_{Eg}$, and p-wave $\eta^{1,2,3}_{T_{1u}}$ OPs under an incident circularly polarized microwave beam at approximately one quarter of the microwave cycle, $t/T \approx 0.25$, where T is the period of the microwave. Coordinates on the thin film are given in units of ξ.

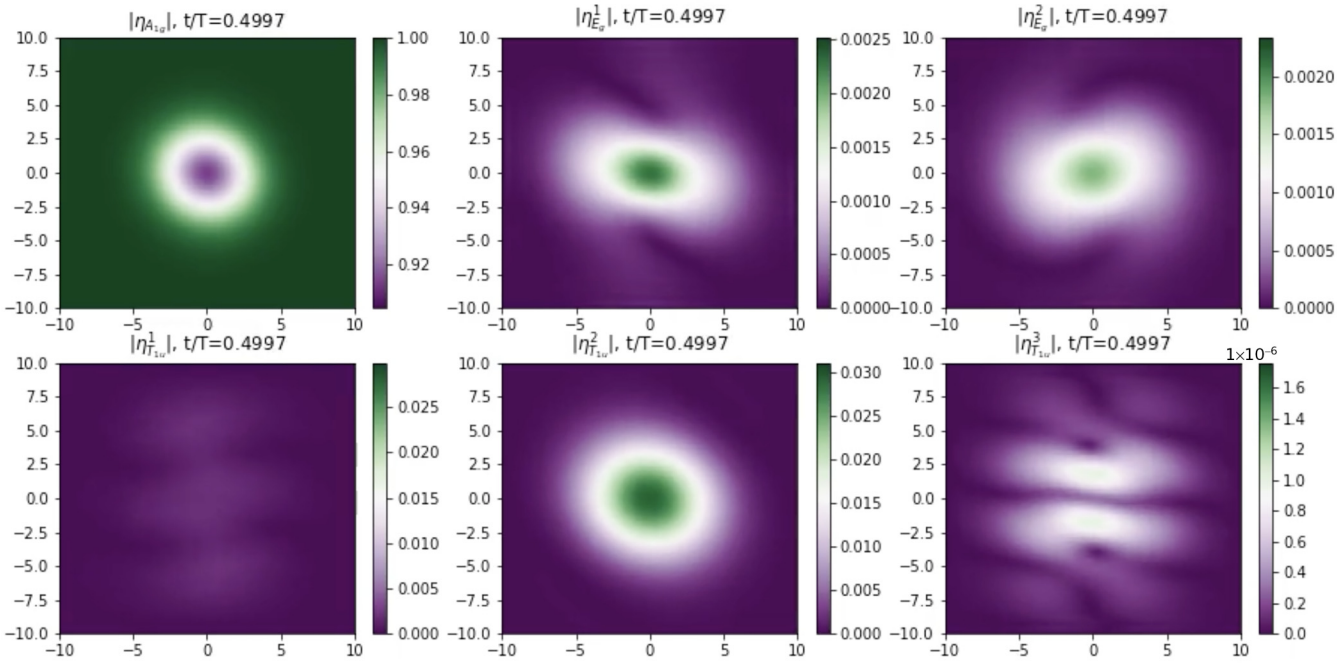


FIG. 10. Density plots for the absolute values of s-wave $\eta_{A_{1g}}$, d-wave $\eta^{1,2}_{Eg}$, and p-wave $\eta^{1,2,3}_{T_{1u}}$ OPs under an incident circularly polarized microwave beam at approximately half of the microwave cycle, $t/T \approx 0.5$, where T is the period of the microwave. Coordinates on the thin film are given in units of ξ.

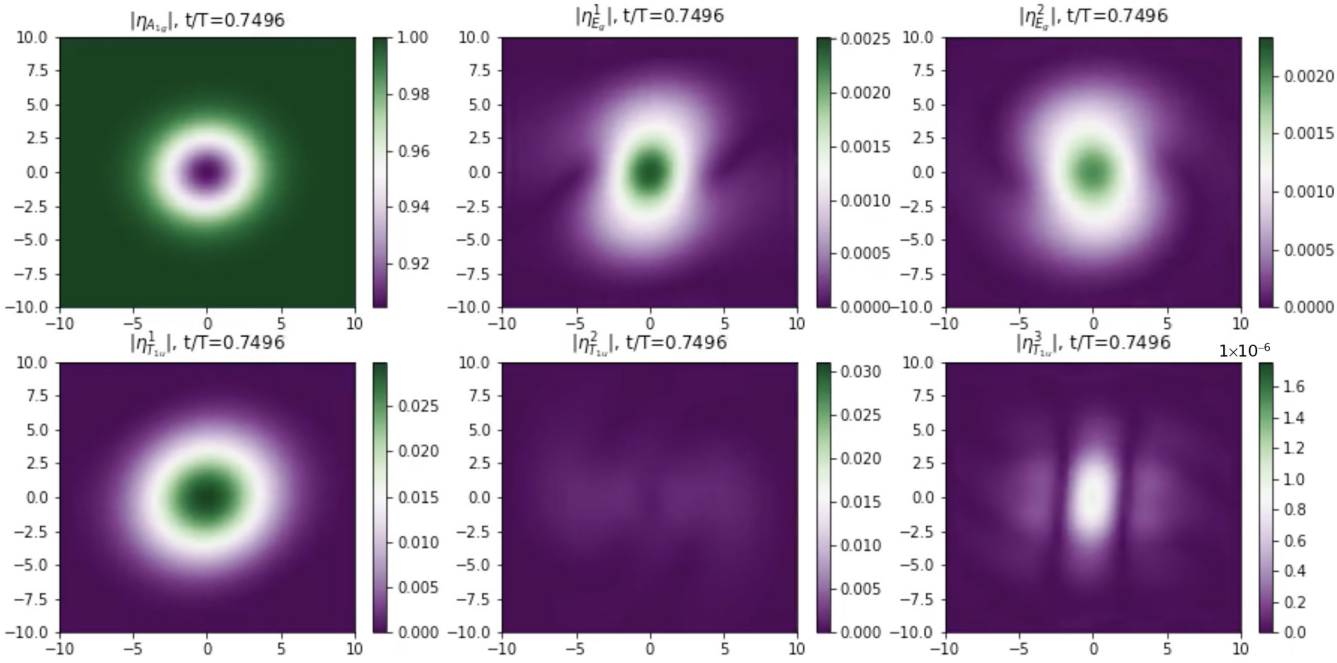


FIG. 11. Density plots for the absolute values of s-wave $\eta_{A_{1g}}$, d-wave $\eta^{1,2}_{Eg}$, and p-wave $\eta^{1,2,3}_{T_{1u}}$ OPs under an incident circularly polarized microwave beam at approximately three quarters of the microwave cycle, $t/T \approx 0.75$, where T is the period of the microwave. Coordinates on the thin film are given in units of ξ.

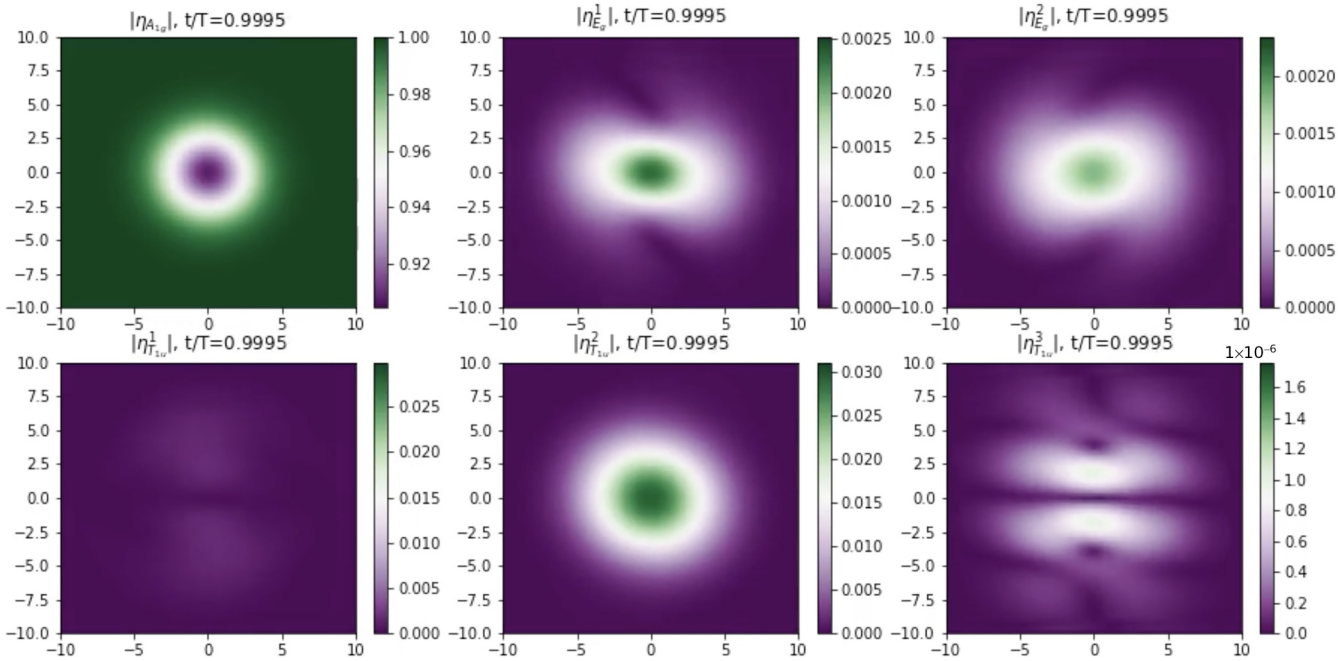


FIG. 12. Density plots for the absolute values of s-wave $\eta_{A_{1g}}$, d-wave $\eta^{1,2}_{Eg}$, and p-wave $\eta^{1,2,3}_{T_{1u}}$ OPs under an incident circularly polarized microwave beam at approximately one full microwave cycle, $t/T \approx 1$, where T is the period of the microwave. Coordinates on the thin film are given in units of ξ.

[1] A. F. G. Wyatt, V. M. Dmitriev, W. S. Moore, and F. W. Sheard, Microwave-enhanced critical supercurrents in constricted tin films, Phys. Rev. Lett. **16**, 1166 (1966).

[2] A. H. Dayem and J. J. Wiegand, Behavior of thin-film superconducting bridges in a microwave field, Phys. Rev. **155**, 419 (1967).

[3] G. M. Eliashberg, Film superconductivity stimulated by a high-frequency field, ZhETF Pis. Red. **11**, 186 (1970) [Sov. JETP Lett. **11**, 114 (1970)].

[4] G. M. Eliashberg and B. I. Ivlev, Theory of superconductivity stimulation, in *Nonequilibrium Superconductivity*, Modern Problems in Condensed Matter Sciences, edited by D. N. Langenberg and A. I. Larkin (North-Holland, Amsterdam, 1986), Chap. 6, Vol. 12, pp. 211–251.

[5] T. Klapwijk and J. Mooij, Microwave-enhanced superconductivity in aluminium films, Phys. B+C **81**, 132 (1976).

[6] J. A. Pals and J. Dobben, Measurements of microwave-enhanced superconductivity in aluminum strips, Phys. Rev. B **20**, 935 (1979).

[7] D. Fausti, R. I. Tobey, N. Dean, S. Kaiser, A. Dienst, M. C. Hoffmann, S. Pyon, T. Takayama, H. Takagi, and A. Cavalleri, Light-induced superconductivity in a stripe-ordered cuprate, Science **331**, 189 (2011).

[8] S. Kaiser, C. R. Hunt, D. Nicoletti, W. Hu, I. Gierz, H. Y. Liu, M. Le Tacon, T. Loew, D. Haug, B. Keimer, and A. Cavalleri, Optically induced coherent transport far above T_c in underdoped $YBa_2Cu_3O_{6+\delta}$, Phys. Rev. B **89**, 184516 (2014).

[9] M. Mitrano, A. Cantaluppi, D. Nicoletti, S. Kaiser, A. Perucchi, S. Lupi, P. Di Pietro, D. Pontiroli, M. Riccò, S. R. Clark, D. Jaksch, and A. Cavalleri, Possible light-induced superconductivity in K_3C_{60} at high temperature, Nature (London) **530**, 461 (2016).

[10] D. Nicoletti and A. Cavalleri, Nonlinear light–matter interaction at terahertz frequencies, Adv. Opt. Photonics **8**, 401 (2016).

[11] M. Buzzi, D. Nicoletti, S. Fava, G. Jotzu, K. Miyagawa, K. Kanoda, A. Henderson, T. Siegrist, J. A. Schlueter, M.-S. Nam, A. Ardavan, and A. Cavalleri, Phase diagram for light-induced superconductivity in κ-$(ET)_2$-X, Phys. Rev. Lett. **127**, 197002 (2021).

[12] A. Komnik and M. Thorwart, BCS theory of driven superconductivity, Eur. Phys. J. B **89**, 244 (2016).

[13] M. A. Sentef, A. F. Kemper, A. Georges, and C. Kollath, Theory of light-enhanced phonon-mediated superconductivity, Phys. Rev. B **93**, 144506 (2016).

[14] M. Knap, M. Babadi, G. Refael, I. Martin, and E. Demler, Dynamical Cooper pairing in nonequilibrium electron-phonon systems, Phys. Rev. B **94**, 214504 (2016).

[15] M. Babadi, M. Knap, I. Martin, G. Refael, and E. Demler, Theory of parametrically amplified electron-phonon superconductivity, Phys. Rev. B **96**, 014512 (2017).

[16] Y. Murakami, N. Tsuji, M. Eckstein, and P. Werner, Nonequilibrium steady states and transient dynamics of conventional superconductors under phonon driving, Phys. Rev. B **96**, 045125 (2017).

[17] R. Shimano and N. Tsuji, Higgs mode in superconductors, Annu. Rev. Condens. Matter Phys. **11**, 103 (2020).
[18] T. Mizushima and M. Sato, Imprinting spiral Higgs waves onto superconductors with vortex beams, Phys. Rev. Res. **5**, L042004 (2023).
[19] D. Kang, S. Kitamura, and T. Morimoto, Quantum optical spanner: Twisting superconductors with vortex beam via Higgs mode, Phys. Rev. B **112**, 214315 (2025).
[20] D. Kang, T.-T. Yeh, T. Morimoto, and A. V. Balatsky, Kapitza-Dirac interference of Higgs waves in superconductors, arXiv:2511.10954.
[21] S. Gassner, C. S. Weber, and M. Claassen, Light-induced switching between singlet and triplet superconducting states, Nat. Commun. **15**, 1776 (2024).
[22] T. Yokoyama, Creation of superconducting vortices by angular momentum of light, J. Phys. Soc. Jpn. **89**, 103703 (2020).
[23] V. D. Plastovets, I. D . Tokman, B. Lounis, A. S. Mel'nikov, and A. I. Buzdin, All-optical generation of Abrikosov vortices by the inverse Faraday effect, Phys. Rev. B **106**, 174504 (2022).
[24] T.-T. Yeh, H. Yerzhakov, L. Bishop-Van Horn, S. Raghu, and A. Balatsky, Quantum printing and induced vorticity in superconductors I: Linearly polarized light, Phys. Rev. Res. **7**, 043111 (2025).
[25] T.-T. Yeh, H. Yerzhakov, L. B.-V. Horn, S. Raghu, and A. Balatsky, Quantum printing and induced vorticity in superconductors II: Laguerre-Gaussian beam, Phys. Rev. Res. **7**, 043112 (2025).
[26] T.-T. Yeh, E. Wilson, M. Fogelström, and A. Balatsky, Light induced Berezinskii-Kosterlitz-Thouless transition in superconducting films, arXiv:2510.22645.
[27] H. Dehghani, M. Hafezi, and P. Ghaemi, Light-induced topological superconductivity via Floquet interaction engineering, Phys. Rev. Res. **3**, 023039 (2021).
[28] S. Kitamura and H. Aoki, Floquet topological superconductivity induced by chiral many-body interaction, Commun. Phys. **5**, 174 (2022).
[29] Z. Shen, C. Xie, W.-C. Chen, and Y. Wang, Light control of triplet pairing in correlated electrons with mixed-sign interactions, Commun. Phys. **8**, 475 (2025).
[30] T. Yokoyama, Floquet engineering triplet superconductivity in superconductors with spin-orbit coupling or altermagnetism, Phys. Rev. B **112**, 024512 (2025).
[31] P.-H. Fu, S. Mondal, J.-F. Liu, Y. Tanaka, and J. Cayao, Floquet engineering spin triplet states in unconventional magnets, Phys. Rev. Lett. **136**, 066703 (2026).
[32] C. L. Kane and E. J. Mele, Quantum spin Hall effect in graphene, Phys. Rev. Lett. **95**, 226801 (2005).
[33] L. D. Landau and E. M. Lifshitz, *Statistical Physics*, Course of Theoretical Physics (Pergamon Press, Oxford, 1969), Vol. 5.
[34] G. Aeppli, A. V. Balatsky, S. Bonetti, G. Cardoso, S. Raghu, E. Syljuåsen, T.-T. Yeh, S.-Z. Lin, Y. Liu, J. Weissenrieder, and P. J. Wong, Quantum printing, arXiv:2509.16792.
[35] V. V. Kabanov, Triplet pairing and upper critical field in the mixed state of d-wave superconductors, Phys. Rev. B **76**, 172501 (2007).
[36] E. Persky, A. V. Bjørlig, I. Feldman, A. Almoalem, E. Altman, E. Berg, I. Kimchi, J. Ruhman, A. Kanigel, and B. Kalisky, Magnetic memory and spontaneous vortices in a van der Waals superconductor, Nature (London) **607**, 692 (2022).
[37] S. Mandal and C.-X. Liu, Pair-mixing induced time-reversal-breaking superconductivity, Phys. Rev. B **114**, 094511 (2026).
[38] M. Sigrist and K. Ueda, Phenomenological theory of unconventional superconductivity, Rev. Mod. Phys. **63**, 239 (1991).
[39] J. F. Annett, Symmetry of the order parameter for high-temperature superconductivity, Adv. Phys. **39**, 83 (1990).
[40] M. Sigrist, Introduction to unconventional superconductivity, AIP Conf. Proc. **789**, 165 (2005).
[41] B. Normand, H. Kohno, and H. Fukuyama, Properties of a mixed-symmetry superconductor, Phys. C **235–240**, 2275 (1994).
[42] C. O'Donovan and J. Carbotte, Mixed order parameter symmetry in the BCS model, Phys. C **252**, 87 (1995).
[43] M. P. Sörensen, T. Schneider, and M. Frick, Nonlinear properties of the BCS gap equation, in *Microscopic Aspects of Nonlinearity in Condensed Matter*, edited by A. R. Bishop, V. L. Pokrovsky, and V. Tognetti (Springer, Boston, 1991), pp. 315–327.
[44] J. Hutchinson and F. Marsiglio, Mixed temperature-dependent order parameters in the extended Hubbard model, J. Phys.: Condens. Matter **33**, 065603 (2021).
[45] P. Senarath Yapa, X. Guo, J. Maciejko, and F. Marsiglio, Mixed-symmetry superconductivity and the energy gap, Phys. C **633**, 1354719 (2025).
[46] V. P. Mineev and K. V. Samokhin, Helical phases in superconductors, Zh. Eksp. Teor. Fiz. **105**, 747 (1994) [Sov. Phys. JETP **78**, 401 (1994)].
[47] K. V. Samokhin, E. S. Zijlstra, and S. K. Bose, $CePt_3Si$: An unconventional superconductor without inversion center, Phys. Rev. B **69**, 094514 (2004).
[48] V. P. Mineev and K. V. Samokhin, Nonuniform states in noncentrosymmetric superconductors: Derivation of Lifshitz invariants from microscopic theory, Phys. Rev. B **78**, 144503 (2008).
[49] K. V. Samokhin, Gradient energy of superconductors without inversion symmetry, Phys. C **489**, 19 (2013).
[50] A. Kapustin and L. Radzihovsky, Piezosuperconductivity: Novel effects in noncentrosymmetric superconductors, Phys. Rev. B **105**, 134514 (2022).
[51] T. Kamatani, S. Kitamura, N. Tsuji, R. Shimano, and T. Morimoto, Optical response of the Leggett mode in multiband superconductors in the linear response regime, Phys. Rev. B **105**, 094520 (2022).
[52] R. Nagashima, S. Tian, R. Haenel, N. Tsuji, and D. Manske, Classification of Lifshitz invariant in multiband superconductors: An application to Leggett modes in the linear response regime in Kagome lattice models, Phys. Rev. Res. **6**, 013120 (2024).
[53] A. Dunbrack, P. Virtanen, and T. T. Heikkilä, Quantum geometry of time-reversal symmetry breaking in flat-band superconductivity, Phys. Rev. B **113**, 174525 (2026).
[54] P. W. Atkins, M. S. Child, and C. S. G. Phillips, *Tables for Group Theory* (Oxford University Press, Oxford, 1970).
[55] G. Katzer, Character table for the O_h point group, http://gernot-katzers-spice-pages.com/character_tables/Oh.html.
[56] L. Landau and E. Lifshitz, *Quantum Mechanics: Non-Relativistic Theory*, Course of Theoretical Physics (Butterworth-Heinemann, Oxford, 1981).

[57] A. Talkachov, P. Leask, and E. Babaev, Multiple correlation lengths and type-1.5 superconductivity in $U(1)$ superconductors due to hidden competition between irreducible representations of nonlocal pairing, Phys. Rev. B **113**, 224520 (2026).

[58] N. B. Kopnin, *Theory of Nonequilibrium Superconductivity* (Oxford University Press, Oxford, 2001), Vol. 110.

[59] L. Kramer and R. J. Watts-Tobin, Theory of dissipative current-carrying states in superconducting filaments, Phys. Rev. Lett. **40**, 1041 (1978).

[60] R. J. Watts-Tobin, Y. Kröhenböhl, and L. Kramer, Nonequilibrium theory of dirty, current-carrying superconductors: Phase-slip oscillators in narrow filaments near T_c, J. Low Temp. Phys. **42**, 459 (1981).

[61] L. Landau and E. Lifshitz, *Mechanics* (Elsevier, Amsterdam, 1982), Vol. 1.

[62] A. Samoilenka and E. Babaev, Microscopic derivation of superconductor-insulator boundary conditions for Ginzburg-Landau theory revisited: Enhanced superconductivity at boundaries with and without magnetic field, Phys. Rev. B **103**, 224516 (2021).

[63] P.-G. D. Gennes, *Superconductivity of Metals and Alloys* (CRC Press, Boca Raton, FL, 2018).

[64] C. Caroli, P. G. de Gennes, and J. Matricon, Sur certaines propriétés des alliages supraconducteurs non magnétiques, J. Phys. Radium **23**, 707 (1962).

[65] A. A. Abrikosov, Concerning surface superconductivity in strong magnetic fields, Zh. Eksp. Teor. Fiz. **47**, 720 (1964) [Sov. Phys. JETP **20**, 480 (1965)].

[66] A. Sergeev and V. Mitin, Electron-phonon interaction in disordered conductors: Static and vibrating scattering potentials, Phys. Rev. B **61**, 6041 (2000).

[67] M. Sidorova, A. Semenov, H.-W. Hübers, K. Ilin, M. Siegel, I. Charaev, M. Moshkova, N. Kaurova, G. N. Goltsman, X. Zhang, and A. Schilling, Electron energy relaxation in disordered superconducting NbN films, Phys. Rev. B **102**, 054501 (2020).

[68] J.-X. Zhu, W. Kim, C. S. Ting, and C.-R. Hu, Time-dependent Ginzburg-Landau equations for mixed $d-$ and s-wave superconductors, Phys. Rev. B **58**, 15020 (1998).

[69] S. Gassner (private communication).

[70] H. Yerzhakov, T.-T. Yeh, and A. Balatsky, Induction of orbital currents and Kapitza stabilization in superconducting circuits with Laguerre-Gaussian microwave beams, Phys. Rev. B **110**, 144519 (2024).

[71] https://github.com/hennadii-phys/GeneralizedTDGL_Oh.